

# Plant Volatile Signatures of Growth and Defense during Abiotic Stress

Kolby Jardine<sup>1</sup>, Rebecca Dewhirst<sup>1</sup>, Suman Som<sup>1</sup>, Joseph Lei<sup>1</sup>, Eliana Tucker<sup>1</sup>, Robert Young P<sup>2</sup>, Miguel Portillo-Estrada<sup>3</sup>, Yu Gao<sup>4</sup>, Luping Su<sup>5</sup>, Silvano Fares<sup>6</sup>, Cristina Castanha<sup>1</sup>, and Jenny Mortimer<sup>4</sup>

<sup>1</sup>E O Lawrence Berkeley National Laboratory

<sup>2</sup>Pacific Northwest National Laboratory

<sup>3</sup>Research group PLECO (Plants and Ecosystems) Department of Biology University of Antwerp Wilrijk Belgium

<sup>4</sup>Joint BioEnergy Institute

<sup>5</sup>Tofwerk USA Boulder CO USA

<sup>6</sup>Consiglio Nazionale delle Ricerche

July 19, 2022

## Abstract

Growth suppression and defense signaling are simultaneous strategies that plants invoke to respond to abiotic stress. Here, we show that the drought stress response of poplar trees (*Populus trichocarpa*) is initiated by a suppression in cell wall derived methanol (MeOH) emissions and activation of acetic acid (AA) fermentation defenses. Temperature sensitive emissions dominated by MeOH (AA/MeOH < 30%) were observed from physiologically active leaves, branches, detached stems, leaf cell wall isolations, and whole ecosystems. In contrast, drought treatment resulted in a suppression of MeOH emissions and strong enhancement in AA emissions together with fermentation volatiles acetaldehyde, ethanol, and acetone. These drought-induced changes coincided with a reduction in stomatal conductance, photosynthesis, transpiration, and leaf water potential. The strong enhancement in AA/MeOH emission ratios during drought (400-3,500%) was associated with an increase in acetate content of whole leaf cell walls, which became significantly <sup>13</sup>C 2-labeled following the delivery of <sup>13</sup>C 2-acetate via the transpiration stream. The results are consistent with MeOH and AA production at high temperature in hydrated tissues associated with accelerated primary cell wall growth processes, which are downregulated during drought. Our observations are consistent with drought-induced activation of aerobic fermentation driving high rates of foliar AA emissions and enhancements in leaf cell wall O-acetylation. We suggest that atmospheric AA/MeOH emission ratios could be useful as a highly sensitive signal in studies investigating environmental and biological factors influencing growth-defense trade-offs in plants and ecosystems.

## Plant Volatile Signatures of Growth and Defense during Abiotic Stress

Kolby J Jardine<sup>1\*</sup>, Rebecca A Dewhirst<sup>1</sup>, Suman Som<sup>1</sup>, Joseph Lei<sup>1</sup>, Eliana Tucker<sup>1</sup>, Robert P Young<sup>2</sup>, Miguel Portillo-Estrada<sup>3</sup>, Yu Gao<sup>4</sup>, Luping Su<sup>5</sup>, Silvano Fares<sup>6,7</sup>, Cristina Castanha<sup>1</sup>, Jenny C Mortimer<sup>4,8</sup>

<sup>1</sup> Climate and Ecosystem Science Division, Lawrence Berkeley National Lab, Berkeley, CA 94720, USA (kjgardine@lbl.gov)

<sup>2</sup> Environmental Molecular Sciences Laboratory, Pacific Northwest National Lab, Richland, WA, USA

<sup>3</sup> Research group PLECO (Plants and Ecosystems), Department of Biology, University of Antwerp, Wilrijk, Belgium

<sup>4</sup> Joint BioEnergy Institute, Lawrence Berkeley National Lab, Emeryville, CA USA

<sup>5</sup> Tofwerk USA, Boulder, CO, USA

<sup>6</sup> Institute of BioEconomy, National Research Council, Rome, Italy

<sup>7</sup> Department of Environmental Science, Policy, and Management, University of California at Berkeley, CA USA

<sup>8</sup> School of Agriculture, Food, and Wine, University of Adelaide, Glen Osmond, SA, Australia

**Highlight:** Acetic acid/methanol leaf emissions ratios are a sensitive indicator of the balance between plant growth and defense during drought.

## Abstract

Growth suppression and defense signaling are simultaneous strategies that plants invoke to respond to abiotic stress. Here, we show that the drought stress response of poplar trees (*Populus trichocarpa*) is initiated by a suppression in cell wall derived methanol (MeOH) emissions and activation of acetic acid (AA) fermentation defenses. Temperature sensitive emissions dominated by MeOH (AA/MeOH < 30%) were observed from physiologically active leaves, branches, detached stems, leaf cell wall isolations, and whole ecosystems. In contrast, drought treatment resulted in a suppression of MeOH emissions and strong enhancement in AA emissions together with fermentation volatiles acetaldehyde, ethanol, and acetone. These drought-induced changes coincided with a reduction in stomatal conductance, photosynthesis, transpiration, and leaf water potential. The strong enhancement in AA/MeOH emission ratios during drought (400-3,500%) was associated with an increase in acetate content of whole leaf cell walls, which became significantly <sup>13</sup>C<sub>2</sub>-labeled following the delivery of <sup>13</sup>C<sub>2</sub>-acetate via the transpiration stream. The results are consistent with MeOH and AA production at high temperature in hydrated tissues associated with accelerated primary cell wall growth processes, which are downregulated during drought. Our observations are consistent with drought-induced activation of aerobic fermentation driving high rates of foliar AA emissions and enhancements in leaf cell wall O-acetylation. We suggest that atmospheric AA/MeOH emission ratios could be useful as a highly sensitive signal in studies investigating environmental and biological factors influencing growth-defense trade-offs in plants and ecosystems.

## Keywords and Abbreviations:

Acetic acid (AA), aerobic fermentation, methanol (MeOH), AA/MeOH ratio, cell wall esters, pectin, xylan, plant drought stress, growth suppression, volatile organic compounds (VOCs)

## Introduction

Terrestrial ecosystem dynamics are dramatically changing in response to trends in surface warming and drought (Palut and Canziani, 2007). Increased magnitude, frequency, and spatial distribution of abiotic stress anomalies threaten the ability of natural and managed ecosystems to produce sustainable food, wood, biofuels, and other bioproducts as well as to mitigate increased atmospheric CO<sub>2</sub> by photosynthetic conversion to biomass. Driven by increasing leaf-atmosphere vapor pressure deficits and soil moisture limitations (Eamus et al., 2013), partial stomatal closure in response to high temperature and drought stress reduces leaf gas exchange including net photosynthesis and transpiration fluxes (Dewhirst et al., 2021a). This phenomenon is well documented on diurnal time scales in numerous ecosystems, where a mid-day depression of net photosynthesis, transpiration, and stomatal conductance are associated with high vapor pressure deficits and leaf temperatures above their optimal values (Pathre et al., 1998).

Prolonged excessive water loss via transpiration not replaced by water uptake from the soil can result in drought-induced tissue senescence and mortality, thereby converting individual plants and ecosystems from net sinks of CO<sub>2</sub> to net sources (McDowell et al., 2008; Jardine et al., 2015; Liu et al., 2021). In northern China, trees of the fast growing genus poplar, which are actively being investigated for afforestation efforts and as renewable sources of biofuels and bioproducts globally, have experienced large-scale dieback and

mortality in recent years (Ji et al., 2020). An estimated 79.5% of the area of the poplar forests have experienced severe degradation with an observed trend of narrower tree-ring widths of intact trees together with reduced soil moisture. These observations highlight the need to understand the mechanisms of poplar forest growth suppression and die-back in response to drought stress (Ji et al., 2020).

A common thread among many of the biochemical and physiological processes that determine ecosystem dynamic responses to climate change variables are alterations in plant cell wall chemical composition, structure, and function (Dewhirst et al., 2020a). A large proportion of the plant cell wall polymers can be heavily modified with methyl and *O*-acetyl ester groups which may play important roles in cell growth and tissue development (Peaucelle et al., 2012), proper xylem (Yuan et al., 2016) and stomatal functioning (Amsbury et al., 2016), central carbon and energy metabolism (Jardine et al., 2017), and stress communication and signaling (Novaković et al., 2018). For example, wood of hybrid poplar trees, one of the fastest growing temperate trees in the world, is composed of lignin (22%), cellulose (40%), hemicellulose (20%) dominated by the *O*-acetylated polysaccharide glucuronoxylan, and other polysaccharides such as pectins (18%), which can be both heavily *O*-acetylated and methyl-esterified (Sannigrahi et al., 2010). The two main components of the plant primary cell wall, the pectin matrix and the cellulose/xyloglucan network, are constantly being remodeled to support dynamic morphological and physiological processes from daily growth and stress response patterns, to developmental changes over longer time scales (Chebli and Geitmann, 2017). This remodeling is regulated, in part, by a number of loosening and stiffening agents including pectin and xylan methyl and acetyl esterases which catalyze the hydrolysis of cell wall esters on the wall. The hydrolysis of methyl and *O*-acetyl esters leads to rapid physicochemical changes in the cell wall and the release of methanol (Fall, 2003) and acetic acid (Scheller, 2017). Given that cell wall methyl and *O*-acetyl esters are known to modify cell wall elasticity/rigidity (Peaucelle et al., 2011), and previous observations have shown links between bulk cell wall elasticity and water relations (Roig-Oliver et al., 2020), they may play important roles in the response to drought (Ganie and Ahammed, 2021). However, how the degree of cell wall esterification varies with abiotic stress is largely unknown (Pauly and Keegstra, 2010; Gille and Pauly, 2012).

One evolutionarily conserved, but poorly understood survival strategy in plants is drought-induced activation of aerobic fermentation, resulting in the formation of acetate (Kim et al., 2017). The degree of acetate accumulation in plants predicts survivability, in part by mediating protein acetylation and jasmonate defense signaling. In this study, we hypothesize that due to hydraulic limitations to growth during drought, cell wall-derived MeOH production is inhibited. Moreover, although cell wall-derived AA may be an important source of foliar AA emission to the atmosphere (Dewhirst et al., 2020b), we hypothesize that aerobic fermentation becomes the dominant source of leaf AA emissions during drought, as a central component of the plant drought response. We aimed to define real-time patterns in MeOH and AA emissions together with the fermentation volatiles acetaldehyde, ethanol, and acetone in parallel with leaf gas exchange (net photosynthesis, transpiration, stomatal conductance) and leaf water potential during experimental drought stress in 2-year old potted California poplar (*Populus trichocarpa*) trees and complementary MeOH and AA gas exchange studies on leaf bulk cell wall preparations and physiologically active leaves, branches and whole ecosystems.

We define the AA/MeOH emission ratio as a potentially sensitive atmospheric indicator of environmental and biological conditions that favor rapid plant growth versus reduced growth and defense activation. Using detached branches and whole plant xylem delivery of a 10 mM<sup>13</sup>C<sub>2</sub>-acetate solution via the transpiration stream followed by analysis of <sup>13</sup>C<sub>2</sub>-acetate content of leaf cell walls preparations, we evaluate the hypothesis that aerobic fermentation signaling can impact the acetylation of numerous biopolymers including cell wall carbohydrates.

## Materials and Methods

### Leaf physiological impacts during an experimental drought

Thirty California poplar (*Populus trichocarpa*) saplings were obtained from a commercial supplier (Plants

of the Wild, USA). The trees were transferred into #2 pots (6.59 L) with Supersoil planting media (Scotts Co., USA) and maintained for two years in the UC Berkeley Oxford Tract greenhouse under natural lighting supplemented with LED lighting (6:00–20:00 light period; Lumigrow 325 Pro, USA). The thirty potted trees reached a stem diameter (5 cm) and height (1.5 m) just prior to the commencement of experimental measurements. A subsection (15 individuals) of the 2-year old trees had water withheld for one week (drought plants), while a control group (15 individuals) continued to receive normal watering patterns. For each individual throughout the controlled drought experiment, one mature leaf was selected for leaf gas exchange measurements in the greenhouse using a portable Li6800 photosynthesis system including stomatal conductance ( $g_s$ , mol m<sup>-2</sup> s<sup>-1</sup>), net photosynthesis ( $A$ , μmol m<sup>-2</sup> s<sup>-1</sup>), and transpiration ( $E$ , mmol m<sup>-2</sup> s<sup>-1</sup>) under standard environmental conditions (400 ppm reference CO<sub>2</sub>, 25 mmol mol<sup>-1</sup> reference absolute humidity, 1000 μmol m<sup>-2</sup>s<sup>-1</sup> photosynthetically active radiation, 600 μmol s<sup>-1</sup> leaf chamber air flow rate, 31 °C heat exchange block). Immediately following leaf gas exchange measurements in the morning, leaf water potential was determined using a nitrogen pressure chamber instrument (Model 600, PMS Inst., USA). The leaf was detached from the tree using a razor blade, and the petiole sealed in the leaf pressure chamber where nitrogen pressure slowly increased until liquid water was visible from the petiole. Following the gas exchange and leaf water potential measurements, a second mature leaf was taken from each of the 30 trees and frozen on dry ice and stored at -80°C prior to cell wall analysis. Leaf gas exchange and water potential measurements and frozen leaf samples were collected from one mature leaf for each of the 15 control and 15 drought-treated individuals at time = 0, 1, 4, and 7 days.

#### Leaf Alcohol Insoluble Residue (AIR) preparations

Cell wall preparations (alcohol insoluble residue; AIR), were created from poplar leaf samples collected during the drought and <sup>13</sup>C<sub>2</sub>-acetate labeling experiments. Leaves were flash frozen in liquid nitrogen and then ground to a powder with a pestle and mortar on dry ice. The ground samples were incubated in 96% (v/v) ethanol at 70°C for 30 minutes. The supernatant was discarded and the samples washed successively in 100% ethanol, 2:3 chloroform: methanol (twice, with shaking for at least 1 hour), 60% ethanol, 80% ethanol and 100% ethanol. Samples were centrifuged and the supernatant discarded between each washing step. The resulting AIR was dried in a speedvac and destarched for the monosaccharide analyses using amylase, amyloglucosidase and pullulanase (Megazyme Ltd., Ireland) as previously described (Sechet *et al.*, 2018).

Bulk *O*-acetyl ester content of AIR samples was carried out using a commercial kit (Acetate Assay Kit, BioVision, CA, USA). AIR samples (2.5 mg) were saponified with NaOH (1 M, 125 μL) for 16 hours then neutralized with 1 M HCl. The samples were centrifuged (10 minutes at 15000 rpm) and 5 μL of the supernatant was transferred to a 96-well plate. The samples were treated with the assay kit enzymes and plates incubated at room temperature for 40 mins. Absorbances were measured at 450 nm on a 96-well plate reader (SpectraMax M2; Molecular Devices, CA, USA). Total *O*-acetyl content of the AIR samples (μg/mg AIR) were determined by including a six-point calibration on each plate using the included standard.

In order to determine bulk leaf cell wall monosaccharide composition, destarched AIR (200 μg) was incubated in 2M trifluoroacetic acid (400 μl) at 120°C for 3 hours. The supernatant was collected after centrifugation. The pellet was washed with 200 μl milliQ water, centrifuged and the supernatant collected. The combined supernatants from each sample were dried in a speedvac. The sample was resuspended in 200 μl milliQ water, filtered on a 0.22 μm centrifuge filtration plate then analyzed for monosaccharide composition using high-pressure anion-exchange chromatography (Dionex-ICS 5000, Dionex, CA, USA).

#### Real-time AA and MeOH emission measurements

Experimental details of the leaf, branch, and ecosystem gas exchange methods to determine AA and MeOH emissions, as well as the detached stem, detached leaf, and hydrated AIR temperature response curves can be found in the supplementary methods. Briefly, emission rates of MeOH and AA were quantified in real-time (roughly 2.5 measurements per minute) using a high sensitivity quadrupole proton transfer reaction mass spectrometer (PTR-MS, Ionicon, Innsbruck Austria, with a QMZ 422 quadrupole, Balzers, Switzerland). The PTR-MS was regularly calibrated to a primary standard by dynamic dilution (Supplementary **Figure**

**S1** ). AA and MeOH emissions were determined using PTR-MS at the leaf level using an environmentally controlled leaf photosynthesis system (Model 6800, Licor Biosciences, USA), branch level using a custom 5.0 L transparent Tedlar gas exchange enclosure with artificial lighting, and from a temperature-controlled chamber used for detached leaf, stem, and hydrated AIR AA and MeOH emission studies (Model 150 Dynacalibrator, +/- 0.01 C temperature accuracy, Vici Metronics, USA). Together with air temperature, continuous above canopy ambient AA and MeOH concentrations during the growing season were made at a poplar plantation in Belgium (Portillo-Estrada *et al.*, 2018), a mixed hardwood forest in Alabama (Suet *et al.*, 2016), and above a citrus grove in California (Park *et al.*, 2013). Vertical ecosystem fluxes of MeOH and AA were estimated at the Belgium field site using the technique of eddy covariance employing high frequency vertical wind and MeOH and AA concentration measurements (Portillo-Estrada *et al.*, 2018). While ecosystem concentration and flux measurements MeOH were collected at all three sites using eddy covariance with PTR-TOF-MS, only the Belgium poplar plantation reported ecosystem scale AA flux data. At the Alabama mixed forest site, AA fluxes were not reported (Suet *et al.*, 2016) and at the citrus grove in California, AA fluxes were reported to suffer from inlet dampening of high frequency concentration variations (Park *et al.*, 2013). This loss of AA flux signal was explained by dampening of fast fluctuations in the sample tube due to stickiness of AA with respect to the inert tubing walls. Therefore, at the Alabama and California sites, diurnal ambient concentrations of MeOH and AA were analyzed instead of fluxes as a function of air temperature.

### Long-distance<sup>13</sup>C<sub>2</sub>-acetate transport in the transpiration stream and leaf cell wall O-acetylation interactions

In order to evaluate the possibility of long-distance metabolic interactions between plant tissues mediated by acetate in the transpiration stream, including influencing O-acetylation dynamics of cell walls, <sup>13</sup>C<sub>2</sub>-acetate labeling studies were carried out on individual *P. trichocarpates* transferred from the greenhouse to the laboratory. <sup>13</sup>C<sub>2</sub>-acetate delivery to leaves was accomplished using detached branches (N = 3 branches, 1 branch/individual) placed in a 10 mM solution of sodium <sup>13</sup>C<sub>2</sub>-acetate (Sigma-Aldrich, USA) for 2 days inside an environmentally controlled growth chamber (Percival Intellus Control System, USA) maintained at 27.5 °C daytime temperature (6:00–20:00; 30% light) and 23 °C nighttime temperature (20:00–6:00). After 2 days, the branches took up roughly 30–40 ml of the <sup>13</sup>C<sub>2</sub>-acetate -acetate solution. In addition, a single individual of 2.1 m height was placed in the laboratory under automated daytime lighting with continuous daytime (150 µl min<sup>-1</sup>) and nighttime (70 µl min<sup>-1</sup>) xylem injection at the base of the stem with a 10 mM sodium <sup>13</sup>C<sub>2</sub>-acetate acetate solution (1,176 ml injected over 7 days using a flow controlled M6 Pump, Valco Instruments Co. Inc., USA). Following the <sup>13</sup>C<sub>2</sub>-acetate -acetate labeling period (branch: 2 day, tree: 7 day), a mature leaf was removed and flash frozen under liquid nitrogen and stored at -80 °C before isolating whole leaf cell walls through the generation of AIR. Leaf AIR samples were also prepared from detached branches fed with water and 10 mM acetate with natural <sup>13</sup>C/<sup>12</sup>C abundance as controls. Experimental details of the AIR saponification followed by <sup>13</sup>C-labeling analysis of the released acetate can be found in the supplementary methods.

## Results

### Leaf gas exchange and water potential responses to experimental drought

Following the cessation of soil moisture additions on Day 0, large impacts on leaf water use and CO<sub>2</sub> metabolism could already be observed by Day 1 of the drought (**Figure 1** ). For example, mean stomatal conductance (g<sub>s</sub>) values of drought treated plants declined from 1.1 mol m<sup>-2</sup> s<sup>-1</sup> on day 0 to 0.026 mol m<sup>-2</sup> s<sup>-1</sup>, representing a 97% decrease. These low conductance values were maintained throughout the drought treatment on day 4 and 7. As expected from a strong drought-induced decrease in g<sub>s</sub>, leaf gas exchange of CO<sub>2</sub> and H<sub>2</sub>O in the light showed a large suppression in drought treated plants. Under standard environmental conditions, average net photosynthesis (A) decreased from 13.4 µmol m<sup>-2</sup> s<sup>-1</sup> on Day 0 to -0.5 µmol m<sup>-2</sup> s<sup>-1</sup> on Day 1, representing a 104% decrease and loss of net carbon assimilation. These near zero and often negative net CO<sub>2</sub> assimilation values continued in the drought plants through days 4 and 7. Likewise, leaf transpiration (E) decreased by 94% on Day 1 as a result of the experimental drought treatment with average values declining from 5.7 mmol m<sup>-2</sup> s<sup>-1</sup> on Day 0 to 0.33 mmol m<sup>-2</sup> s<sup>-1</sup> on Day 1. These low leaf transpiration

values continued through Days 4 and 7. The strong reduction in  $g_s$ , A, and E observed during on Days 1, 4, and 7 in drought treated individuals was associated with a decrease in leaf water potential ( $LWP$ ), indicating dehydration of the leaves. Average  $LWP$  declined from  $-0.56$  MPa in drought treated leaves on Day 0 to  $-1.0$  on Days 1, 4, and 7, representing a 79% decline. After the drought treatment, despite daily soil moisture additions resuming for the droughted trees, all the trees lost their leaves.

#### Branch MeOH and AA emission responses to experimental drought

During the drought experiment, a subset of drought ( $N = 6$ ) and control ( $N = 6$ ) plants were transported to the analytical laboratory in the morning and analyzed for ‘snap-shot’ branch MeOH and AA emissions for 1 hour in a constant light and temperature environment (**Fig. 2a-c**). Control plants had high average rates of MeOH emissions ( $2.3-4.4$   $\text{nmol m}^{-2} \text{s}^{-1}$ ) and low, but detectable levels of AA emissions ( $0.1$   $\text{nmol m}^{-2} \text{s}^{-1}$ ). In contrast, drought stressed trees showed low MeOH emissions ( $0.3$   $\text{nmol m}^{-2} \text{s}^{-1}$ ) while also showing higher average AA emissions ( $0.2$   $\text{nmol m}^{-2} \text{s}^{-1}$ ). This pattern resulted in the branch ‘snap-shot’ AA/MeOH emission ratio for the control ( $10 \pm 10\%$ ) being lower than the drought stressed plants ( $84 \pm 57\%$ ).

In contrast to the greenhouse drought experiments which showed rapid negative leaf physiological effects. A second set of drought experiments occurred in a cooler lab, where limited lighting was provided artificially via a grow-light. To confirm the pattern of decreased MeOH emissions and increased AA emissions, and consequently high AA/MeOH emission ratios during the greenhouse drought, real-time MeOH and AA emissions were characterized before, during and after the onset of drought impacts on leaf gas exchange. Five well-watered control individuals were sequentially transported to the laboratory and studied for real-time diurnal branch VOC emissions in the absence of additional soil moisture additions under a daytime (6:00-22:00) light pattern that mimicked the greenhouse lighting conditions. While variability in the timing and magnitudes of the MeOH and AA emissions was observed between the five individuals, the same general emission pattern was observed during the real-time emission studies as those from the ‘snap-shot’ studies with drought inducing a pattern of decreasing branch MeOH emissions and increasing AA emissions together with high AA/MeOH emissions ratios (**Figure 2d-f**, **Figure 3** and supplementary **Figures S2-5**).

When the temporal patterns of branch gas exchange during drought was analyzed in more detail, four distinct phases could be described. The first ‘growth phase’ with physiologically active foliage is characterized by high rates of transpiration, net photosynthesis, and MeOH emissions, with low AA emissions and values of AA/MeOH emission ratios  $< 30\%$  (e.g. the first three days in **Figure 3**). During this ‘growth phase’, high light-dependent emissions of isoprene linked with photosynthetic  $\text{CO}_2$  assimilation occur during the day (6:00-22:00). Despite the constant daytime light environment and relatively stable laboratory temperature, a strong circadian gas exchange pattern was observed with maximum gas exchange fluxes near mid-day of transpiration (enhancing  $\text{H}_2\text{O}$  concentrations in the branch chamber), net photosynthesis (drawing down the  $\text{CO}_2$  concentrations in the branch chamber), and MeOH and AA emissions. However, the high MeOH emissions relative to AA emissions from physiologically active branches in the ‘growth phase’ constrain daytime AA/MeOH emission ratios to low values, reaching maximum mid-day values of 6% (e.g. day 3 in **Figure 4**). The second phase of drought response consists of a strong suppression in MeOH emissions, apparently occurring prior to any reductions in stomatal conductance and  $\text{CO}_2$  and  $\text{H}_2\text{O}$  gas exchange (e.g. day 4 in **Figure 3**). Although AA emissions remained low, similar to the well-watered active growth conditions, branch AA/MeOH emission ratios during this ‘MeOH suppression’ phase increased slightly from 18% on day 4 to 24% on day 5. The third phase of plant response to drought stress is characterized by a reduction in stomatal conductance with a suppression of transpiration and net photosynthesis rates, a continued strong suppression of MeOH emissions, together with the activation of aerobic fermentation including high branch emissions of the fermentation volatiles acetaldehyde, ethanol, acetic acid (AA), and acetone (e.g. initiated on day 5 in **Figure 3**). High rates of fermentation VOC emissions were found to be initiated both during the day and the night, depending on the individual, and so is not directly considered a light-dependent process. Emissions of acetaldehyde during this phase was far higher than those of the other fermentation products, whose emissions in general tracked the rise and fall of acetaldehyde emissions in this fermentation phase. Elevated branch fermentation VOC emissions from the individual shown in **Figure 3**

continued for three days, with the peak in AA/MeOH emission ratio (444%) occurring on beginning of day 6. Throughout this ‘aerobic fermentation’ phase, daytime transpiration and net photosynthesis continued to decline, likely as a consequence of decreasing stomatal conductance, with a loss of positive net carbon assimilation evident by day 7 and strongly reduced daytime isoprene emissions. Following this ‘fermentation phase’, a final ‘senescence phase’ was observed (day 7-10), likely associated with irreversible damage to cellular components including photosynthetic membranes and greatly compromised cellular structure and function. In this senescence phase which inevitably resulted in the leaves dying and falling off the tree, isoprene emissions were essentially eliminated, while MeOH emissions increased again to a high level with AA emissions also continuing at an elevated rate resulting in AA/MeOH emission ratios declining but remaining elevated reaching a low value of 50% by day 10.

To test for the potential reversibility of the branch MeOH emission suppression during drought, when another drought-stressed potted tree showed strong suppression of MeOH emissions in the laboratory, re-watering of the soil with 100 ml additions on day 4 (red arrows in supplementary **Figure S6**), resulted in a rapid (~15 min) return of high branch MeOH emissions and a dramatic reduction of the AA/MeOH emission ratios to around 1%. As the soil continued to dry through the experiment, the suppression of MeOH emissions was again rapidly relieved by a 100 ml soil moisture addition, regardless if it was added during the day or night. This watering effect of the drought stressed plant, completely altered the normal diurnal cycle in MeOH emissions which normally peak around mid-day in well-watered individuals. While the drought-stimulated aerobic fermentation emissions were observed on day 5, they were greatly reduced with maximum AA/MeOH emission ratios of 12%. This is in contrast to the five trees for which water was completely withheld (**Figure 3** and **S2-5**) which showed strong drought-stimulated aerobic fermentation emissions and high maximum AA/MeOH emission ratios ranging from 400-3500%.

#### Leaf MeOH and AA emission responses to CO<sub>2</sub>, light, and temperature

In order to evaluate the effect of environmental conditions on well hydrated poplar branches at the leaf level, MeOH and AA emissions, AA/MeOH ratio, stomatal conductance ( $g_s$ ), transpiration, and net photosynthesis ( $P_{net}$ ) measurements occurred in parallel during CO<sub>2</sub>, light, and temperature leaf response studies. To minimize leaf water stress, poplar branches were detached, recut under water, with the target leaf placed in the chamber and the rest of the branch placed in a hydrated atmosphere in the dark. In this way, leaf hydration was maximized by shutting down transpiration from all leaves on the branch except the leaf inside the dynamic leaf chamber. Across the CO<sub>2</sub> ( $A_{net}$ -C<sub>i</sub>, **Fig. 4a-c**), light ( $A_{net}$ -PAR, **Fig. 4d-f**), and temperature ( $A_{net}$ -leaf temp., **Fig. 4g-i**) response curves, MeOH and AA emissions generally tracked patterns of  $g_s$  and E, and did not appear to be strongly dependent on  $A_{net}$ . For example, at low C<sub>i</sub>, MeOH emissions tended to increase with  $g_s$  and decrease with  $g_s$  at high C<sub>i</sub>. However, during the light curves,  $g_s$  values remained high and increased only slightly as a function of PAR, while MeOH and AA emissions also remained relatively stable. In contrast, as leaf temperature increased,  $g_s$  increased up to 35-37 °C before declining at higher temperatures, while MeOH and AA emissions together with transpiration generally increased up to the highest leaf temperatures (40 °C). While  $g_s$  continued to decline in the dark at 40 °C, leaf dark respiration caused  $A_{net}$  to quickly drop to negative values. In contrast, MeOH and AA emissions did not show a fast decline in the dark, but rather declined more gradually together with  $g_s$  and E. Importantly across C<sub>i</sub> and PAR response curves, leaf AA/MeOH emission ratios remained relatively stable with maximum values < 10%. In contrast, AA/MeOH emission ratios increased as a function of temperature reaching maximum values in the light at 40 °C of 10-20%.

Temperature sensitivities of MeOH and AA emissions and AA/MeOH emission ratios from physiologically active trees, detached stems and leaves, hydrated AIR, and whole ecosystems

To better understand the role of temperature in potentially enhancing AA/MeOH emission ratios, the air temperature sensitivities of MeOH and AA emission rates were characterized from branches of well-watered poplar trees, detached stems and leaves, and whole ecosystems. Well-watered poplar trees were individually placed in a growth chamber with diurnally changing air temperature (**Figure 5**). At night in the dark (20:00-6:00), considerable branch transpiration was observed together with relatively high MeOH emissions,

and low to undetectable AA emissions. Under constant daytime (6:00-20:00) light conditions, net positive CO<sub>2</sub> assimilation occurred. As observed at the leaf level, branch transpiration together with MeOH and AA emissions were strongly coupled to the diurnal pattern of air temperature, reaching maximum fluxes during the early afternoon peak in air temperature of 27 °C at 14:00. MeOH emissions were greater than AA emissions at all air temperatures by roughly a factor of 10, except for 1 hour following light to dark transitions where a short burst in AA emissions were observed. Outside of this light-dark period, branch AA/MeOH emission ratios remained low and increased as a function of air temperature from 0-12% (**Figure 5**). A high temperature sensitivity of MeOH and AA emissions from detached poplar branch segments were also observed. Emissions of MeOH and AA and water loss from detached stem segments in the dark increased with temperature from 30-50 °C (Supplementary **Figure S7**). Similar to physiologically active leaves and branches, emissions were dominated by MeOH, resulting in AA/MeOH emission ratios below 12%. Similar temperature sensitivities of MeOH and AA emissions were also obtained from hydrated whole leaf cell wall preparations (alcohol insoluble residue, AIR). Gas-exchange analysis under controlled temperature with hydrated AIR in porous Teflon tubes showed rapid equilibration of MeOH and AA emissions at each chamber temperature in the dark (**Figure 6**). MeOH and AA steady state emissions from hydrated AIR samples increased as a function of temperature from 30-50 °C and were completely dependent on the presence of liquid water interacting with AIR. Similar to physiologically active leaves (**Figure 4**), branches (**Figure 5**), and detached stems (Supplementary **Figure S7**), emissions from hydrated AIR were dominated by MeOH with AA/MeOH emission ratios increasing slightly with temperature but remaining below 30%.

In contrast to AA/MeOH emission ratios from physiologically active leaves, branches, detached stems, and hydrated leaf AIR samples which remained less than 30%, AA/MeOH emission ratios from drought stressed poplar branches were high ranging from 400-3,000% (**Figures 2-3, Supplementary Figures S2-S5**). Similarly, detached poplar leaves placed into the temperature-controlled chamber in the dark in a dry air stream, showed a similar pattern of suppressed MeOH emissions together with temperature stimulated emissions of the fermentation volatiles acetaldehyde, ethanol, acetic acid, and acetone (**Figure 7**). Acetaldehyde emissions peaked at 42.5 °C, AA emissions peaked at 47.5 °C, and the AA/MeOH emission ratio reached a maximum of 2,500% at 45 °C.

We extended our analysis of the temperature sensitivities of AA and MeOH leaf emissions at the ecosystem scale at the Lochristi poplar plantation in Belgium and a mixed hardwood forest in Alabama. Likely due to the very low ambient temperatures at night in Belgium during the growing season (averaging around 15 °C), no significant night time AA concentration or vertical flux was observed (**Figure 8a,b**). In contrast, night-time MeOH emissions of 10 µmol ha<sup>-1</sup>day<sup>-1</sup> and ambient concentrations of 0.5 ppb were detected. Similar to emissions from physiologically active poplar leaves (**Figure 4**) and branches during the day (**Figure 5**), average ecosystem emission rates of AA and MeOH during the 2015 growing season showed a clear diurnal pattern reaching maximum values in the afternoon together with air temperature. AA emissions and ambient concentrations closely followed diurnal increases in air temperature with both reaching a maximum in the afternoon (16:30). In contrast, MeOH emissions peaked around midday (12:00), and this pattern resulted in the AA/MeOH emission and concentration ratios peaking in the early evening (17:30). Ecosystem AA/MeOH emission ratios increased as a function of air temperature from a low of 28% in the early morning to 158% in the afternoon (**Figure 8b**). Likewise, AA/MeOH concentration ratios also increased as a function of air temperature from a low value of 41% in the early morning to 188% in the afternoon (**Figure 8a**).

We also analyzed ambient concentration time series of AA and MeOH as a function of ambient temperature above a mixed forest canopy in Alabama, USA and a citrus grove in California. Similar to the poplar plantation in Belgium, ambient concentrations of AA and MeOH above the mixed forested canopy in Alabama and citrus grove in California followed strong diurnal patterns tightly coupled with air temperature, with air temperature having a positive impact on AA/meOH ambient concentration ratios (**Figure 9**). While ambient concentrations increased during the day relative to the night in the Alabama site (**Figure 9a**) in a similar way to the Belgium site (**Figure 8a**), ambient concentrations decreased during the day at the California site (**Figure 9b**). This may be related to a shallow boundary layer at night where emissions are concentrated, followed by a rapid increase in the boundary layer height during the day due to increased

turbulent mixing. In addition, the site had the highest ambient concentrations of AA (3.6-5.6 ppb) when compared with the Belgium and Alabama sites. Despite the high ambient backgrounds and dilution effect due to turbulent mixing during the day, the MeOH/AA concentration ratio at the California grove increased linearly with air temperature from a low of 19% at night to 29% in the afternoon. This is comparable to the pattern at the Alabama mixed hardwood forest site where MeOH/AA concentration ratios also increased linearly with air temperature from < 5% during early mornings below 20 °C, to high values of 25% during afternoon air temperatures up to 32 °C. Given that the MeOH/AA concentration ratios increased with temperature, but remained below 30%, these values are comparable to AA/MeOH temperature sensitivities observed in the hydrated AIR, leaf, and branch poplar studies.

#### Changes in cell wall composition and esterification patterns in response to drought stress

In order to investigate the potential source(s) of MeOH and AA emissions from poplar leaves and evaluate potential impacts of drought stress on the cell wall polysaccharide composition, leaf bulk monosaccharide composition was determined from AIR samples. Consistent with the expected high pectin content of rapidly expanding leaf primary cell walls, monosaccharide content of AIR from control poplar leaves was dominated by galacturonic acid (GalA, **Figure 10a**). While the monosaccharide content, and by extension polysaccharide content of the cell walls remained largely unchanged during drought, we observed an increase in *O*-acetyl ester content during drought (**Figure 10b**). AIR from control leaves released an average of 0.69  $\mu\text{g g}^{-1}$  of free acetate following saponification which increased by 10% to 0.76  $\mu\text{g g}^{-1}$  of free acetate  $\text{g}^{-1}$  from drought stressed leaves. Leaf AIR *O*-acetyl ester content increased throughout the drought, reaching a maximum after 7 days (**Figure 10b**). After 7 days, the leaves were fully desiccated, and subsequently detached from the tree.

#### Evaluating acetate in the transpiration stream as a substrate for cell wall *O*-acetylation

In order to evaluate potential mechanisms involving rapid changes in cell wall *O*-acetylation in response to drought stress, experiments investigating the long-distance transport of doubly- $^{13}\text{C}$ -labeled  $^{13}\text{C}_2$ -acetate in the transpiration stream of detached branches and a whole intact tree were carried out. To evaluate leaf cell wall *O*-acetylation responses to  $^{13}\text{C}_2$ -acetate in the transpiration stream, cell wall preparations (AIR) were isolated from canopy leaves, and saponified with deuterated sodium hydroxide (NaOD) to quantitatively hydrolyze the esters. The resulting solution was analyzed for acetate isotopologues including monoisotopic acetate ( $^{12}\text{C}_2$ -acetate) and acetate with one ( $^{13}\text{C}$ -1-acetate,  $^{13}\text{C}$ -2-acetate), and two- $^{13}\text{C}$ -atoms ( $^{13}\text{C}_2$ -acetate), by one-dimensional  $^1\text{H}$ -NMR (**Figure 11**).

Acetate released upon saponification of the AIR (from 10 mg dried AIR/mL 0.4M NaOD) ranged in concentration between 212-333 nmol/mg AIR (dry wt.), corresponding to 2.12 mM and 3.33 mM. The concentration of acetate in the method blank was 0.006 mM and, to quantify any additional free acetate that may have been present, incubations of AIR in only  $\text{D}_2\text{O}$  were also carried out. Free acetate was only quantifiable in two detached branch leaf samples at (1.2 and 1.4 nmol/mg AIR (dry wt.), or 0.012 mM and 0.014 mM. In the spectra of the other AIR  $\text{D}_2\text{O}$  incubations, signals from lysine, which were not observed in the saponified AIR, prevented detection and quantitation of acetate. In the two cases where it was quantifiable, the highest amount of free acetate in the AIR amounted to less than 0.7 % of the total concentration of acetate observed after saponification with 0.4 M NaOD.

The isotopologue distributions were determined from the experimental spectra (**Figure 11**) by integrating the peak areas corresponding to each isotopologue and dividing by the sum of the integrated areas of all acetate peaks. The results are summarized in **Table 1** as the fraction of isotopologue divided by its expected fraction at natural abundance wherein a value of 1 indicates no change. In leaf cell AIR, there was an increase in the  $^{13}\text{C}_2$ -acetate isotopologue by a factor of 125 +/- 31 above its expected fraction at natural abundance along with concomitant decreases in the fractions corresponding to the remaining isotopologues. For example, no significant changes or slight decreases were detected in the relative abundances of mono-labeled  $^{13}\text{C}$ -1-acetate and  $^{13}\text{C}$ -2-acetate isotopologues. An increase in the fraction of  $^{13}\text{C}_2$ -acetate isotopologue by a factor of 48 +/- 7 was also observed in two of the three canopy leaf samples collected following one week of 10

mM<sup>13</sup>C<sub>2</sub>-acetate solution continuously injected into the xylem of an intact potted tree. Although branch emissions of <sup>13</sup>C<sub>2</sub>-AA were not observed during the whole tree <sup>13</sup>C<sub>2</sub>-acetate xylem injections, leaf and branch level emissions of <sup>13</sup>C<sub>2</sub>-AA could be observed in some of the experiments (e.g. supplementary **Figure S8**), confirming the delivery of the labeled acetate to the leaves.

## Discussion

Fast growing poplar trees are increasingly being utilized as a sustainable source of bioproducts and biofuels as well as carbon farming, urban greening, hillslope stabilization, and marginal land restoration and reforestation (Ragauskas *et al.*, 2006; Furtado *et al.*, 2014). Field observations have consistently shown that non-water limited poplar plantations have high growth and productivity rates, but are highly sensitive to drought (Ji *et al.*, 2020). Understanding the biological mechanisms and environmental thresholds that determine plant responses to drought stress is critical for predicting how the structure and function of managed ecosystems will respond to environmental change (McDowell *et al.*, 2008). Previous studies have characterized the sequence of plant hydraulic, physiological, biochemical, and structural changes associated with reversible and irreversible responses to drought stress. For example, leaf dehydration responses of ten angiosperm species showed stomatal closure and a decrease in xylem conductance occurring first as a reversible response (Trueba *et al.*, 2019). This was followed by reaching the turgor loss point, xylem embolism, and the cessation of transpiration as a critical irreversible threshold following which further irreversible damage occurred including to the membranes, pigments, and other components of the photochemical system in the chloroplast (Trueba *et al.*, 2019). While ecosystem response to water deficit can be detected by current remote sensing methods such as solar induced fluorescence (SIF) (Sun *et al.*, 2015), and various normalized vegetation indices such as the Normalized Difference Vegetation Index (NDVI) (Peters *et al.*, 2002) and Enhanced Vegetation Index (EVI) (Aulia *et al.*, 2016), these generally only identify extreme drought and the associated irreversible loss of major leaf function such as transpiration and net carbon assimilation. For example, in 2-yr old *Populus deltoides* individuals, while strong responses of net photosynthesis and stomatal conductance to initial water stress were observed at the leaf level, SIF showed relatively minimal changes (Helmet *et al.*, 2020). It was concluded that the value of SIF as an accurate estimator of net photosynthesis may decrease during mild stress events of short duration, especially when the response is primarily stomatal and not fully coupled with the degradation of photosynthetic capacity. This highlights the need for new methods to better understand the biochemical, physiological, and ecological mechanisms *in situ* associated with the onset of drought stress including processes that alter plant growth and defense balances and their associated changes in leaf CO<sub>2</sub> and H<sub>2</sub>O gas exchange fluxes.

In this study, we present foliar AA/MeOH emission ratios as non-invasive gas-phase chemical observational method providing insights into the dynamics of growth and defense processes during abiotic stress from cell wall leaf isolations, individual leaves, branches, and whole ecosystems. We observed 4 potentially distinct phases during the drought response in poplar trees, with unique CO<sub>2</sub>/H<sub>2</sub>O gas exchange, volatile emissions (MeOH and AA), and cell wall characteristics including:

- 1) **Growth Phase:** Well hydrated leaves characterized by high rates of net photosynthesis ( $A_{net}$ ), transpiration ( $E$ ) and stomatal conductance ( $g_s$ ), and less negative leaf water potential ( $LWP$ ) values. MeOH and AA emissions increase with temperature, with AA/MeOH emission ratios low with values below 30%.
- 2) **Methanol Suppression Phase:** Characterized by high rates of  $A$ ,  $E$  and  $g_s$ . Leaf MeOH emissions are suppressed and AA emissions remain low. The ratio of AA/MeOH may increase relative to the growth phase but remain below 30%. Drought effects reversible.
- 3) **Aerobic fermentation Phase** Reduction in  $A_{net}$ ,  $E$ ,  $g_s$ , and MeOH emissions, with high and sustained emissions of the fermentation volatiles acetaldehyde, acetic acid (AA), ethanol, and acetone. Cell wall *O*-acetylation increases and the ratio of AA/MeOH greatly increases to 400-3,500%. Drought effects may or may not be reversible.
- 4) **Senescence Phase:**  $A_{net}$ ,  $E$ ,  $g_s$  close to zero indicating a loss of functional photosynthetic capacity and irreversible degradation of cellular structural integrity. The ratio of AA/MeOH emissions begins to decline from the aerobic fermentation phase, but remains high (e.g. 50-100%).

Pectin, Methanol, and the Growing Plant Cell Wall

The polysaccharide pectin can account for up to 35% of the primary cell wall in dicots and non-grass monocots, and up to 5% of wood tissues (Mohnen, 2008). Newly synthesized pectin in the primary cell wall is known to be highly methyl esterified, with changes in the degree of pectin methylesterification mediated by pectin methylesterases (PME) known to regulate cell wall mechanical properties like elasticity. The degree of pectin methylesterification can have profound impact on physiological processes like tissue morphogenesis and growth as well as numerous biological functions (Levesque-Tremblay *et al.*, 2015). Cell wall synthesis is coupled to changes in cell wall elasticity mediated by pectate formation following pectin demethylesterification (Peaucelle *et al.*, 2012). In *Arabidopsis*, increases in tissue elasticity in living meristems correlated with pectin demethylesterification (Peaucelle *et al.*, 2011) which is required for the initiation of organ formation (Peaucelle *et al.*, 2008). When pectin demethylation was inhibited, stiffening of the cell walls throughout the meristem was observed which completely blocked the formation of primordia (Peaucelle *et al.*, 2008). Thus, pectin demethylation is a critical process that regulates the direction and speed of cell wall expansion during growth and morphogenesis (Braybrook *et al.*, 2012). Consistent with the view that MeOH emissions from plants into the atmosphere primarily derive from pectin demethylation, numerous studies have revealed that leaf methanol emissions tightly correlate with leaf expansion rates (Hüve *et al.*, 2007) with young rapidly expanding leaves emitting higher fluxes of MeOH than mature leaves (Jardine *et al.*, 2016). Our temperature-controlled gas exchange observations of hydrated leaf bulk cell walls (AIR) provides new direct evidence for pectin demethylation as the dominant source of foliar MeOH emissions. Moreover, purified whole leaf cell walls (AIR) hydrated and placed in a porous Teflon tubes that permit gas exchange showed remarkably similar temperature sensitivities of MeOH and AA emissions (**Figure 6**) as physiologically active leaves (**Figure 4**), branches (**Figure 5**), detached stems (supplementary **Figure S7**), and whole ecosystems (**Figure 8-9**), confirming plant cell walls as an important source of these volatile emissions.

In contrast to growth processes, abiotic stress responses may be associated with increased cell wall fortification through a reduction in pectin demethylation rates mediated by pectin methyl esterase inhibitors (PMEI). For example, abiotic stress may lead to the inhibition of pectin demethylation via enhanced expression of PMEI genes known to be involved in abiotic stress tolerance (Anet *et al.*, 2008; Hong *et al.*, 2010; Ren *et al.*, 2019; Wang *et al.*, 2020a). Recent work on drought response of leaf-succulent *Aloe vera* reported the drought-induced folding of hydrenchyma cell walls involves changes in pectin esterification (Ahle *et al.*, 2019). It was hypothesized that the cell wall folding process during drought may be initiated by a reduction in pectin de-esterification and its associated MeOH production and  $\text{Ca}^{+2}$ -complexation, thereby releasing internal constraints on the cell wall. Thus, we suggest that the strong decrease in observed foliar MeOH emissions during water stress (**Figs. 2, 3, 6**, supplementary **S2-5**) may be related to both  $g_s$  reductions and reduced cell wall de-methylation rates related to increased PMEI activity. We speculate that reductions in tissue water potential leads to the inhibition of pectin methyl ester hydrolysis, MeOH production, and growth.

Results from the leaf-level environmental response curves (**Figure 4**) are consistent with the view that stomatal regulated leaf MeOH emissions are controlled by light-independent, but highly temperature-dependent production associated with growth processes (Harley *et al.*, 2007). Thus, light and  $\text{CO}_2$  are assumed to only indirectly influence leaf MeOH emission rates via changes to  $g_s$ . However, we highlight that reduction of  $g_s$  at high temperatures in well hydrated leaves was often unable to prevent the temperature increase in MeOH and AA emissions (**Figure 4**). Similarly, reductions in  $g_s$  during drought were unable to suppress the emissions of fermentation volatiles like AA (**Figs. 2, 3**, supplementary **S2-5**). While regulated by  $g_s$ , our observations suggest that the large changes in AA/MeOH ratios during growth and drought stress responses are largely due to changes in production rates, with MeOH production declining and AA production increasing during different phases of the drought response (**Figure 3**).

#### Aerobic fermentation in plant drought response

The upregulation of aerobic fermentation in plants is now recognized as an evolutionarily conserved drought survival strategy in plants, with the amount of acetate produced directly correlating to survival (Kim *et al.*, 2017). Drought-induced acetate accumulation promotes *de novo* synthesis of the potent phytohormone

jasmonic acid (JA) and the acetylation of histone H4, which influences the priming of the JA signaling pathway for plant drought tolerance (Kim *et al.*, 2017). Thus, acetate regulates an epigenetic switch of metabolic flux conversion and hormone signaling by which plants adapt to drought. However, destructive measurements are required to evaluate acetate-linked drought responses, limiting the temporal and spatial scales that can be studied. As a consequence, few studies have reported aerobic fermentation rates in plants during drought due to the current method requirements of destructive sampling followed by offline tissue analysis of acetate content (Dewhirst *et al.*, 2021b). In this study, by directly quantifying real-time leaf emissions rates of MeOH together with volatiles intermediates of aerobic fermentation (acetaldehyde, AA, ethanol, acetone), we suggest that growth and aerobic fermentation responses to drought can be studied in real-time from individual leaves to whole ecosystems. At the onset of drought in poplar, large increases in the fermentation volatiles acetaldehyde, acetic acid, ethanol, and acetone were consistently emitted from poplar branches despite reduced stomatal conductance. This suggests that drought-activation of the aerobic fermentation pathway occurred (Kim *et al.*, 2017; Rasheed *et al.*, 2018), with foliar emissions of methyl acetate (Dewhirst *et al.*, 2021b) and acetone (Fall 2003, Jardine *et al.*, 2010) associated with acetate activation to acetyl-CoA (Miller *et al.*, 1954).

During aerobic fermentation, acetate formed from the oxidation of acetaldehyde does not lead to Nicotinamide adenine dinucleotide<sup>+</sup> (NAD<sup>+</sup>) regeneration, as in the case of ethanol production in anoxic tissues like flooded roots (Kreuzwieser *et al.*, 1999). However, while NAD<sup>+</sup> regeneration is considered a critical aspect of fermentation under anoxia, it may be less important during aerobic fermentation where acetate may be a key respiratory substrate, effectively coupling aerobic fermentation with mitochondrial respiration to help meet high energy demands of the cell (Tadege 1997). However, non-fermentative sources of acetaldehyde may be possible during stress, such as the peroxidation of membranes associated with irreversible damage (Jardine *et al.*, 2009).

Our study suggests that there are at least two distinct plant sources of atmospheric AA emissions; hydrolysis of *O*-acetyl groups on the cell wall (**Figure 6**) and the aerobic fermentation pathway (**Figures 3, 7**). AA and MeOH emission patterns of hydrated leaf cell wall isolations (AIR) showed similar temperature sensitivities when compared with physiologically active poplar leaves and branches. Emissions of AA and MeOH increased with temperature, with AA/MeOH tending to slightly increase with temperature but generally remaining below 30%. Similar results were observed at the ecosystem scale, for example in Alabama, where ambient AA and MeOH concentrations and AA/MeOH ratio above a mixed hardwood forest increased with air temperature with AA/MeOH ranging from < 5% during early mornings to high values of 25% in the afternoon. The striking similarities in temperature sensitivities of AA, MeOH, and AA/MeOH emissions from hydrated leaf cell wall material (AIR), leaves, branches, and whole ecosystems provides direct evidence for the cell wall as the main source of foliar MeOH and AA emissions during normal physiological activities. In contrast, drought stress activates a second source of AA emissions via aerobic fermentation, which overwhelms cell wall sources. Together with the decreased MeOH emissions, AA/MeOH ratios increased dramatically (400-3,500%). However, we caution that the use of the AA/MeOH emission ratio as a plant and ecosystem growth and stress indicator is only realistic if net emissions of AA and MeOH occur under natural conditions. While net uptake of atmospheric MeOH has not been demonstrated to our knowledge, limited studies on AA exchange between plants and the atmosphere suggests that under polluted atmospheres with high AA concentrations in the lower troposphere, net uptake of atmospheric AA can occur (Jardine *et al.*, 2011).

Cell wall *O*-acetylation is modified by drought

In this study, we found statistically significant enrichments in *O*-acetyl ester content of bulk leaf cell walls (AIR) in response to drought stress (**Fig. 10b**). In contrast, cell wall monomer composition, which was dominated by galacturonic acid from pectin, changed little over seven days following the cessation of watering (**Fig. 10a**). That leaf AIR monosaccharide content was largely insensitive to drought suggests a slower turnover in monosaccharide cell wall polysaccharides than the fast time scales of days observed for changes in volatile emission signatures and cell wall *O*-acetyl ester content changes (1-7 days). *O*-acetyl-substituents are

present on nearly all cell wall polymers with the exception of cellulose, whereas methyl esters are thought to be primarily associated with pectin (Derbyshire *et al.*, 2007). *O*-acetyl esterification of plant cell walls is known to play important physicochemical, mechanical, and structural roles that serve to minimize degradation while enhancing intermolecular interactions with other wall polymers (Biely, 2012). Studies have shown that cell wall *O*-acetylation of hemicellulose and pectin is critical for proper plant growth and functioning. For example, simultaneous mutations of the acetyl transferase genes *TBL32*, *TBL33* and *TBL29/ESK1* in *Arabidopsis* resulted in a severe reduction in xylan *O*-acetyl level down to 15% that of the wild type, and concomitantly, severely collapsed vessels and stunted plant growth (Yuan *et al.*, 2016). Additional studies demonstrated that *Arabidopsis* plants with defective ESK1 enzymes have a constitutive drought syndrome and collapsed xylem vessels, low hydraulic conductivity along with low *O*-acetylation levels in xylan and mannan, low transpiration rates, high water use efficiency, and dwarfism (Lefebvre *et al.*, 2011; Ramírez *et al.*, 2018). Together with these studies, the observation of enhanced leaf cell wall *O*-acetylation during drought (**Figure 10b**) suggests that polysaccharide *O*-acetylation is important for the proper functioning of vascular tissues under hydraulic stress.

### Acetate as a potential substrate for cell wall O-acetylation

While the mechanisms of methyl esterification of pectin and its de-methylation by PME have been the focus of several studies (Willats *et al.*, 2001; Mohnen, 2008), the mechanisms of how *O*-acetyl groups are transferred to and from cell wall polymers and their role in the life cycle of a plant are poorly understood. Current biochemical models of cell wall esters assume that carbohydrate monomers are heavily *O*-acetylated using acetyl-CoA initially in the Golgi apparatus, exported and incorporated into the growing cell wall, and de-esterified on the wall by esterase enzymes at a later point in the life cycle of the cell in support of numerous physiological and biochemical processes. Acetyl transfer activity from acetyl-CoA to xylo oligomers acceptors has been attributed to Golgi localized TBL acetyl transferases (Zhong *et al.*, 2017). Our observations that delivery of  $^{13}\text{C}_2$ -acetate to the transpiration stream of poplar branches and xylem of a whole tree leads to rapid and significant  $^{13}\text{C}_2$ -labeling of *O*-acetyl esters in leaf cell walls isolations (AIR) supports this biochemical mechanism (**Table 1**).  $^1\text{H-NMR}$  analysis of the acetate released following leaf AIR saponification show that satellite signals corresponding to the  $^{13}\text{C}_2$ -acetate isotopologue were detectable in all three detached branch leaf AIR samples and two of the three whole tree leaf AIR samples which had been treated with 10 mM  $^{13}\text{C}_2$ -acetate via the transpiration stream. In contrast, AIR of leaves labeled with  $^{13}\text{C}_2$ -acetate treated with water instead of NaOD did not show any detectable  $^{13}\text{C}_2$ -acetate in solution, suggesting the acetate was bound to the cell wall material via an ester bond, making it unlikely that the delivered  $^{13}\text{C}_2$ -acetate in the transpiration stream became trapped in the cell wall material, but not esterified.

These results suggest a possible link between the drought-induced increase in foliar AA emissions (e.g. **Figure 3**) and increased *O*-acetylation of leaf cell walls (**Figure 10b**). Thus, in addition to providing acetate for protein acetylation and defense gene regulation (Kim *et al.*, 2017), the activation of aerobic fermentation during drought may also supply acetyl-CoA used in the Golgi prior to incorporation into the cell wall (Gou *et al.*, 2012; Orfila *et al.*, 2012; de Souza *et al.*, 2014). This hypothesis is consistent with previous studies with microsomal preparations of a potato cell suspension culture that were supplied with  $^{14}\text{C}$ -acetyl-CoA found radio-labeled acetate in an esterified form on several polysaccharides, including xyloglucan and pectin (Pauly and Scheller, 2000). Although the mechanisms require further investigation, our study is consistent with cell wall methylation and *O*-acetylation of polysaccharides rapidly responding to environmental conditions, potentially allowing plants the flexibility to dynamically alter growth and defense processes. Our observations are consistent with a coordinated reduction in cell wall de-methyl esterification and growth processes during water stress (resulting in a strong suppression in MeOH production) together with an activation of defense processes including stomatal closure, aerobic fermentation (increasing AA production and emissions), and enhancements in cell wall *O*-acetylation.

### Conclusions and prospects

Although plants are known to activate growth suppression and defense signaling during abiotic stress, the biochemical, physiological, and ecological mechanisms involved are under intense investigation. Of particular

importance is the development of non-destructive *in situ* methods that are able to characterize the onset of reversible and irreversible phases of drought stress including alterations in growth and defense balances and their associated changes in leaf CO<sub>2</sub> and H<sub>2</sub>O gas exchange fluxes. Moreover, although cell walls constitute the majority of plant biomass, little information exists on the impact of abiotic stress on the degree of cell wall methylation and *O*-acetylation, which can change biomass properties and value as a renewable source of biofuel or bioproducts. Therefore, understanding the extent to which these changes occur in woody tissue as it develops could help to understand recalcitrance of biomass when harvested, and the extent to which this is driven by exposure of trees to abiotic stress.

In this study, we show that foliar AA/MeOH emissions ratios are a sensitive indicator of the balance between plant growth and defense during drought which can be studied in real-time from individual leaves to whole ecosystems. We identified the active growth phase associated with rapid biomass accumulation and high rates of leaf gas exchange as highly enriched in MeOH emissions relative to AA. Temperature sensitivity studies of MeOH and AA emissions from isolated leaf cell wall preparations (AIR) showed that these volatiles can be released at high rates directly from hydrated AIR with AA/MeOH ratios and their temperature sensitivities similar to emission observations from physiologically active leaves, branches, and ecosystems under non-drought stressed conditions.

However, drought stress was discovered to activate the reversible suppression of MeOH emissions, potentially linked directly to the inhibition of pectin demethylation and suppression of cell wall expansion and growth. Continued exposure to drought conditions lead to numerous coordinated leaf physiological and biochemical changes including reduced stomatal conductance, the suppression of net photosynthesis and transpiration, and the activation of aerobic fermentation. The simultaneous suppression of MeOH emissions and increase in AA emissions during drought resulted in large increases in AA/MeOH foliar emissions ratios from 400-3,500%. While current methods require destructive sampling, our observations suggest that real-time AA emissions (together with other fermentation volatiles like acetaldehyde, ethanol, and acetate) may represent a new highly sensitive technique to evaluate aerobic fermentation-linked defensive processes during abiotic stress. Moreover, results from <sup>13</sup>C<sub>2</sub>-acetate labeling of the transpiration stream followed by <sup>1</sup>H-NMR analysis of the acetate content of leaf cell wall preparations demonstrates that leaf cell wall *O*-acetylation is highly dynamic may derive from aerobic fermentation via acetate activation to acetyl-CoA. Critical to the understanding of the roles of cell wall esters in plant abiotic stress responses is to elucidate their functional role(s) during drought including impacts on growth, hydraulics, defense signaling, and carbon and energy metabolism. Rapid changes to cell wall methyl and *O*-acetyl ester content during drought may allow plants to quickly respond to environmental signals potentially critical for survival during climate extremes.

## Supplementary Information

The following supplementary methods and data are available online

### Supplementary Methods

- Proton Transfer Reaction-Mass Spectrometry
- Dynamic Branch Gas Exchange Methods
- Dynamic Leaf Gas Exchange Responses to Environmental Variables
- Temperature sensitivities of MeOH and AA emissions from detached leaves, stems, and hydrated AIR
- Temperature sensitivities of MeOH and AA emissions from woody crops and forested ecosystems
- *<sup>1</sup>H-NMR analysis of <sup>13</sup>C-labeling of acetate released from leaf bulk AIR following saponification*

### Supplementary Figures

**Figure S1** : Example PTR-MS calibration to a primary MeOH and AA gas phase standard

**Figures S2-S5** : Biological replicates #2-5 of real-time branch gas exchange dynamics of VOCs, CO<sub>2</sub>, and H<sub>2</sub>O during a drought experiment of potted poplar trees

**Figure S6** : Recovery of drought-suppressed branch MeOH emissions by 100 mL soil moisture additions prior, during, and after the onset of aerobic fermentation during drought

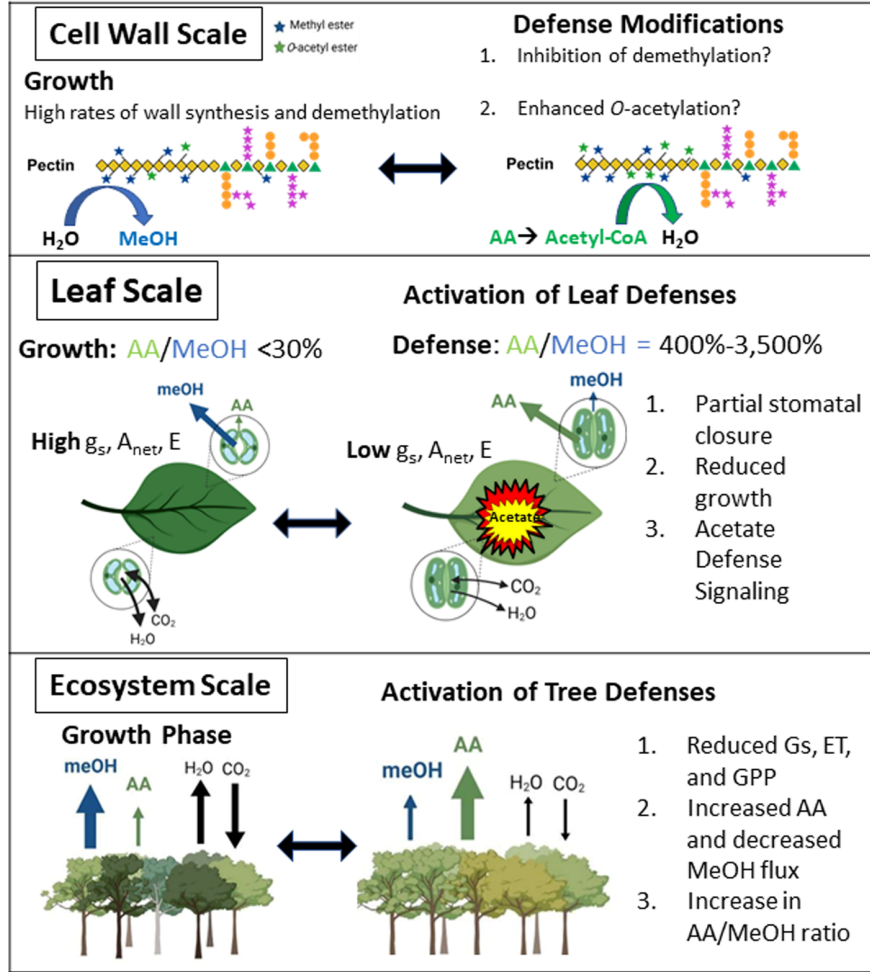
**Figure S7** : Emissions of methanol (MeOH) and acetic acid (AA) as a function of temperature from a detached poplar stem segment in a dark temperature-controlled chamber

**Figure S8** : Leaf  $^{13}\text{C}_2$ -acetic acid emissions during branch  $^{13}\text{C}_2$ -acetate labeling via the transpiration stream

| Leaf sample     | Acetate isotopologue       | $F_{\text{experiment}}/F_{\text{natural abundance}}$ |
|-----------------|----------------------------|--|
| Detached branch | $^{12}\text{C}_2$ -acetate | 0.985 +/- 0.008 (*)                                  |
| Detached branch | $^{13}\text{C}$ -1-acetate | 0.6 +/- 0.3 (ns)                                     |
| Detached branch | $^{13}\text{C}$ -2-acetate | 1.00 +/- 0.09 (ns)                                   |
| Detached branch | $^{13}\text{C}_2$ -acetate | 125 +/- 31 (*)                                       |
| Whole tree      | $^{12}\text{C}_2$ -acetate | 0.995 +/- 0.004 (ns)                                 |
| Whole tree      | $^{13}\text{C}$ -1-acetate | 0.9 +/- 0.2 (ns)                                     |
| Whole tree      | $^{13}\text{C}$ -2-acetate | 1.01 +/- 0.04 (ns)                                   |
| Whole tree      | $^{13}\text{C}_2$ -acetate | 48 +/- 7 (*)   |

**Table 1**  $^1\text{H}$ -NMR isotopologue analysis results for acetate released following saponification of isolated leaf cell wall samples from (a) 3 detached branches (one per tree,  $N = 3$ ) treated with 10 mM  $^{13}\text{C}_2$ -acetate solution for 2 days as well as (b) canopy leaf ( $N = 3$ ) samples from a 2-year old tree following continuous diurnal injections of the 10 mM  $^{13}\text{C}_2$ -solution into the xylem at the base of the tree for 7 days (night: 70  $\mu\text{L}/\text{min}$ , day: 150  $\mu\text{L}/\text{min}$ ). Following saponification of the cell wall isolates, the values were obtained by integrating the area of the free acetate signals (corresponding to each of the four isotopologues shown in **Fig. 10**), and calculating the fraction of each acetate isotopologue to the total ( $F_{\text{experiment}} = \text{peak area acetate isotopologue}/\text{peak area of total acetate isotopologues}$ ), and reporting the ratio of  $F_{\text{exp}}$  to that from natural abundance fractions ( $F_{\text{natural abundance}}$ ). Note, statistically significant changes in  $F_{\text{experiment}}/F_{\text{natural abundance}}$  (\*), no statistically significant changes (ns).

## Figures



**Graphical abstract** : Summary of changes to MeOH and AA emission patterns, cell wall *O*-acetylation, and leaf gas exchange in poplar trees during growth and defense against drought stress from cell walls, leaves, to whole ecosystems.

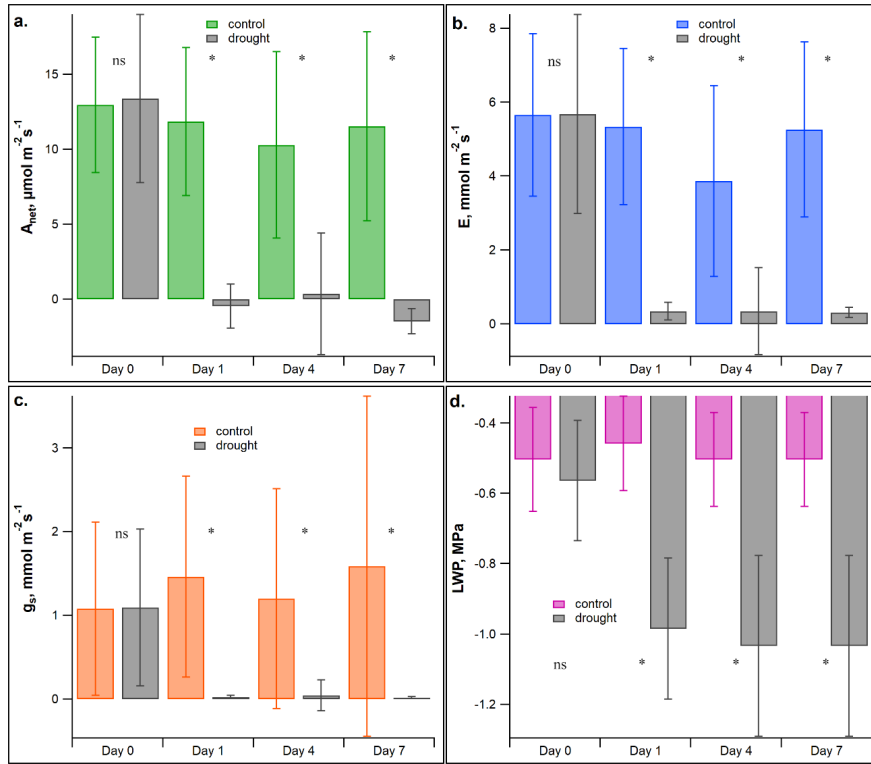


**Figure 1 :** Leaf physiological parameters in control and drought treated plants. Poplar saplings were subject to drought for 7 days. Leaf observations were made on day 0 ( $n = 24$ ), day 1 ( $n = 6$ ), day 4 ( $n = 18$ ), and day 7 ( $n = 18$ ) of (a) Net photosynthesis ( $A_{net}$ ,  $\mu\text{mol m}^{-2}\text{s}^{-1}$ ), (b) transpiration ( $E$ ,  $\text{mmol m}^{-2}\text{s}^{-1}$ ), (c) stomatal conductance ( $g_s$ ,  $\text{mmol m}^{-2}\text{s}^{-1}$ ) and (d) leaf water potential ( $LWP$ , MPa). Values are plotted as average  $\pm$  1 standard deviation (ns indicates no statistical significance between control and drought treatments, \* indicates statistically significant difference,  $P < 0.05$ ).

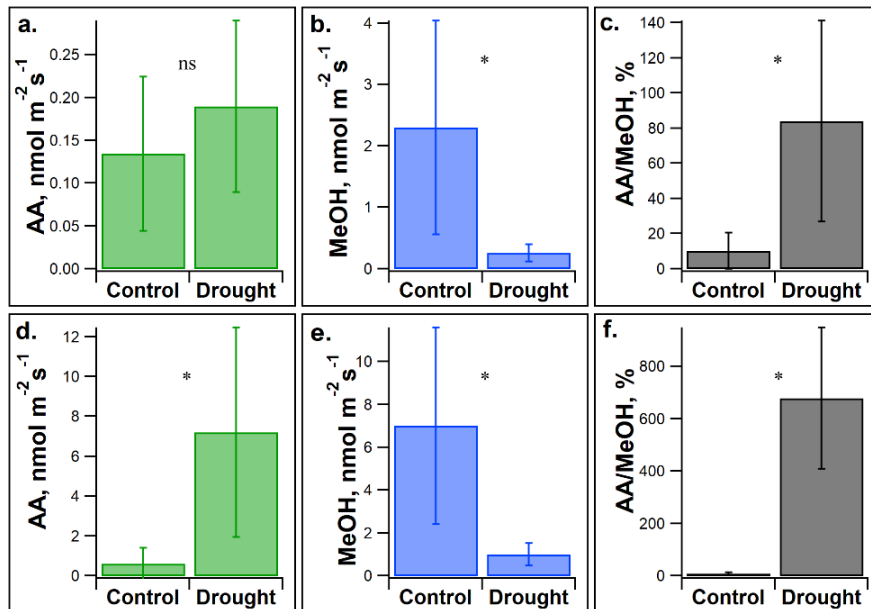


**Figure 2:** Branch daytime ‘snap-shot’ branch emissions of (a) acetic acid (AA), (b) methanol (MeOH), and (c) the AA/MeOH emission ratio from control (N = 21) and drought stressed (N = 16) poplar trees. In addition, the daily maximum (d) AA emissions, (e) MeOH emissions, and (f) AA/MeOH emission ratios from real-time branch gas exchange measurements on the first day of secession of soil water addition (Day = 0: control) and a subsequent day during the drought response at the time where AA emissions were maximized (N = 5) are also shown. All values are plotted as average  $\pm$  one standard deviation (ns indicates no statistical significance between control and drought treatments, \* indicates statistically significant differences,  $P < 0.05$ ).

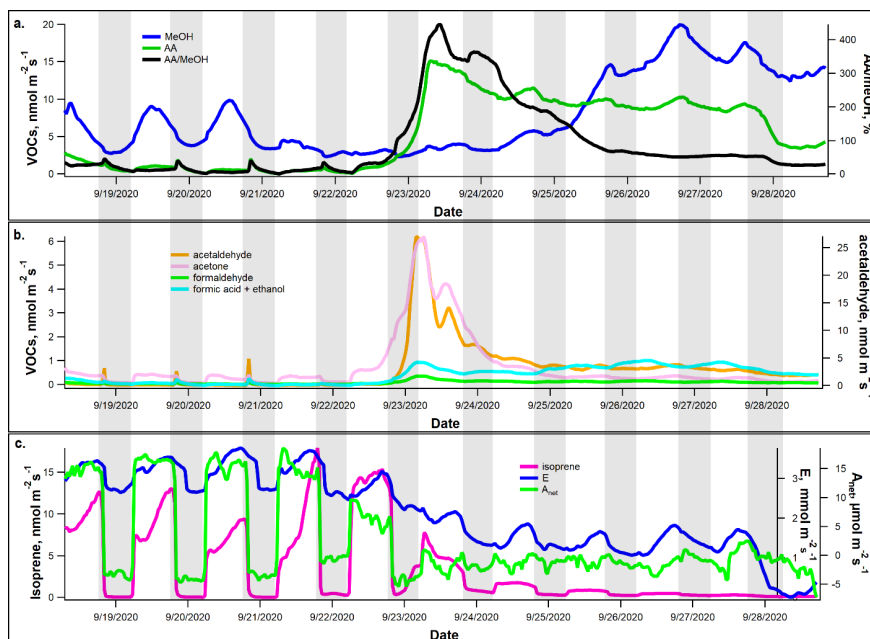


**Figure 3:** Real-time branch emissions of VOCs together with transpiration ( $E$ ,  $\text{mmol m}^{-2} \text{s}^{-1}$ ) and net photosynthesis ( $A_{\text{net}}$ ,  $\mu\text{mol m}^{-2} \text{s}^{-1}$ ) fluxes during a 10-day drought experiment. A branch enclosure was installed on a potted poplar tree and water withheld for the 10-day duration. Daily branch flux patterns of (a) Methanol (MeOH), Acetic Acid (AA), AA/MeOH emission ratio, (b) Aerobic fermentation intermediates (acetaldehyde, ethanol, acetone) (c)  $\text{CO}_2$  and  $\text{H}_2\text{O}$  and the photosynthetic product isoprene. Shaded areas represent the night-time where the grow light was switched off.

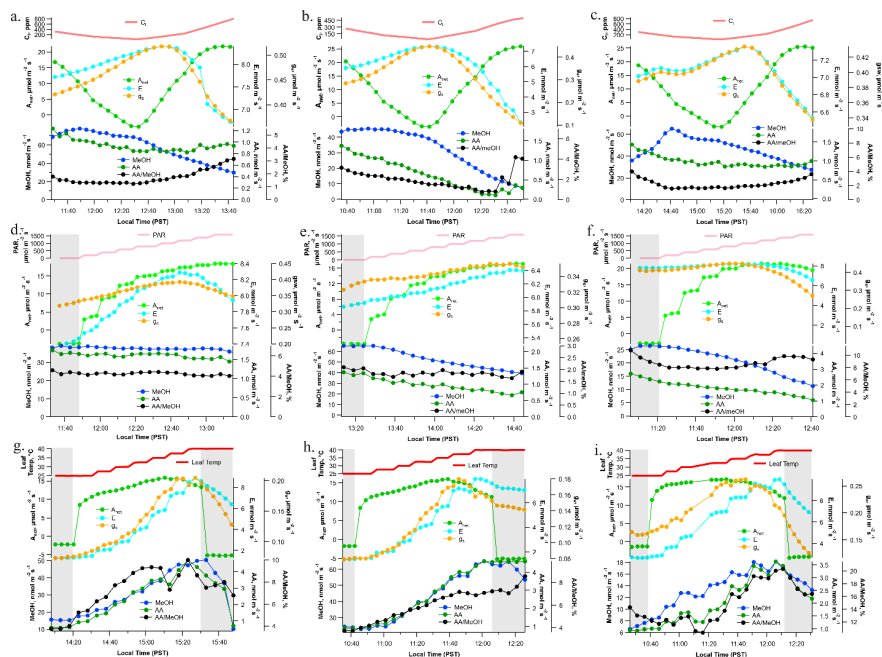


**Figure 4** : Dynamic leaf gas exchange responses of methanol (MeOH), acetic acid (AA), AA/MeOH, net photosynthesis ( $A_{net}$ ), transpiration ( $E$ ), and stomatal conductance ( $g_s$ ) from detached hydrated poplar branches as a function of (a-c) leaf internal  $CO_2$  concentrations ( $C_i$ ), (d-f) incident Photosynthetically Active Radiation (PAR) flux, and (g-i) leaf temperature. Shaded regions indicate dark conditions inside the leaf chamber.

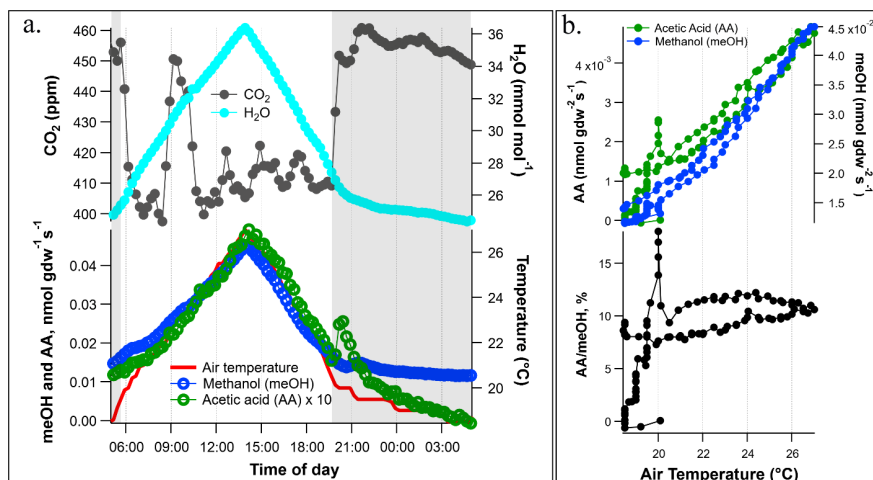


**Figure 5**: (a) Example diurnal pattern of AA and MeOH emissions from a physiologically active poplar branch from a tree inside a growth chamber programmed with a temperature increase during the day under constant illumination. (b) Also shown are AA and MeOH emissions and the ratio of AA/MeOH emissions plotted as a function of air temperature.

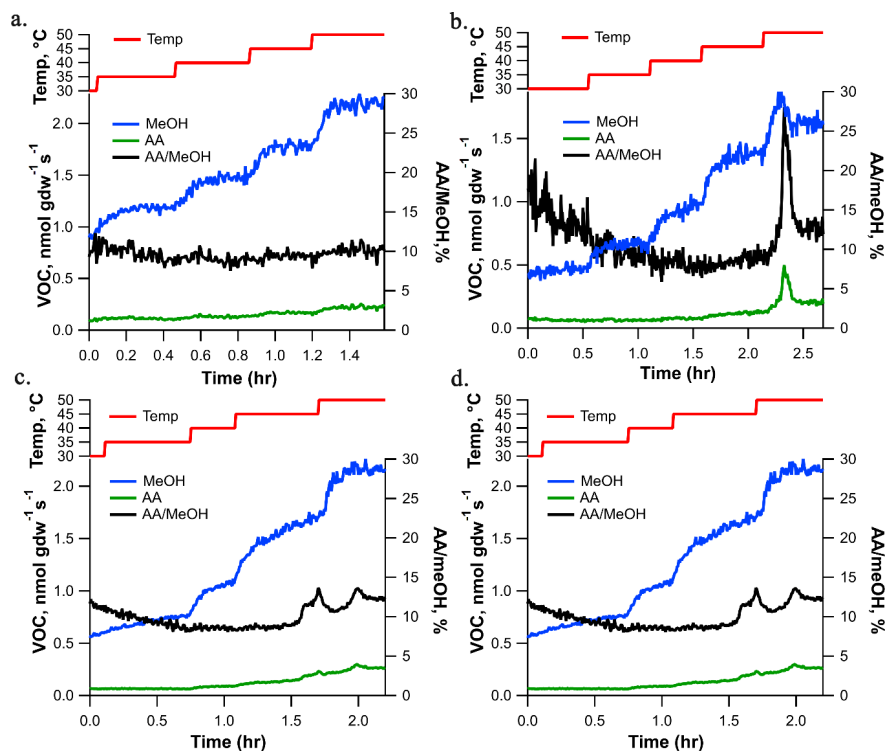


**Figure 6:** Emissions of methanol (MeOH) and acetic acid (AA) as a function of time from hydrated leaf cell wall isolates (AIR) in porous Teflon PTFE diffusion tubes as chamber air temperature increased from 30 °C to 50 °C.

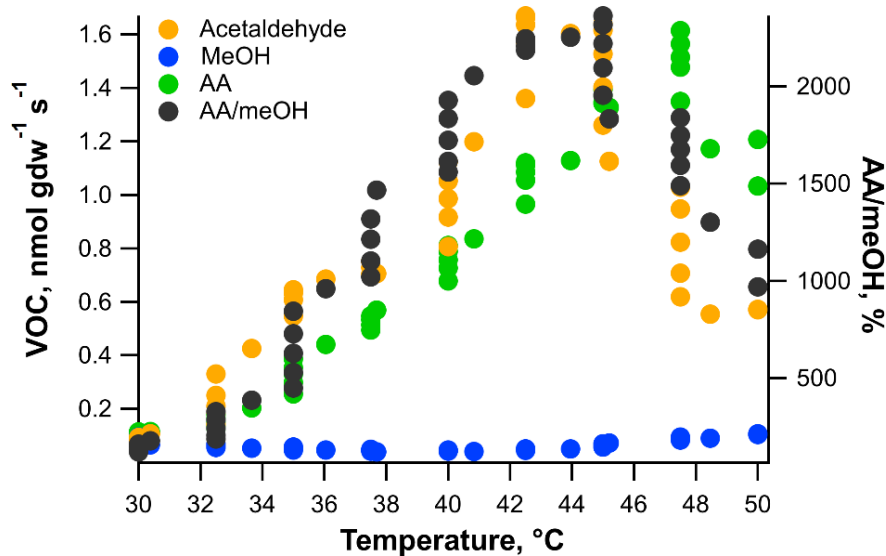


**Figure 7 :** Example Acetaldehyde and Acetic Acid (AA) emissions from a detached poplar leaf in the dark with 1.0 L min dry air passing over in a temperature-controlled chamber (Ethanol and Acetone emissions are not shown for clarity). Average Acetaldehyde, AA, MeOH, and AA/MeOH emission values are plotted at each chamber temperature.

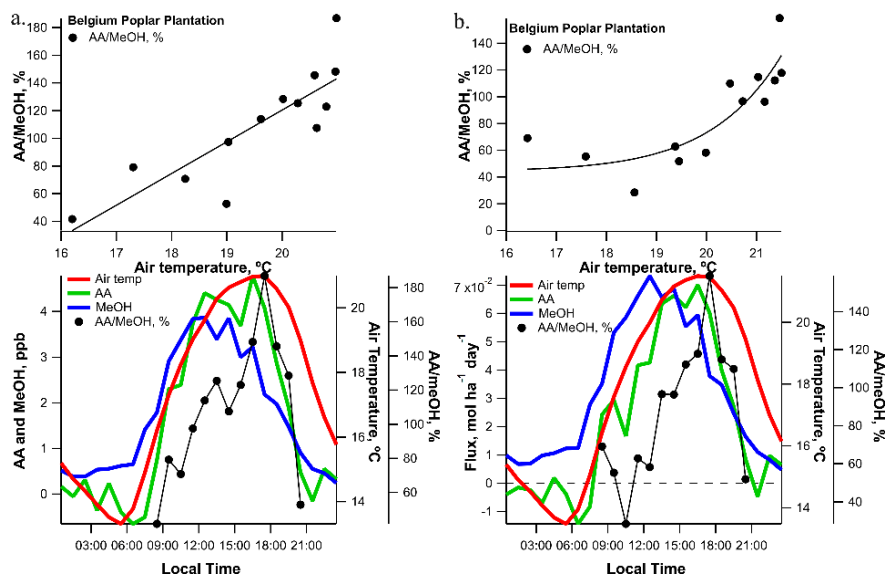


**Figure 8 :** (a) Average diurnal MeOH (blue) and AA (green) (a) ambient concentrations and (b) vertical fluxes together with air temperature above a poplar plantation during the 2015 growing season in Belgium (Portillo-Estrada *et al.*, 2018). Also plotted are average AA/MeOH ratios during the day.

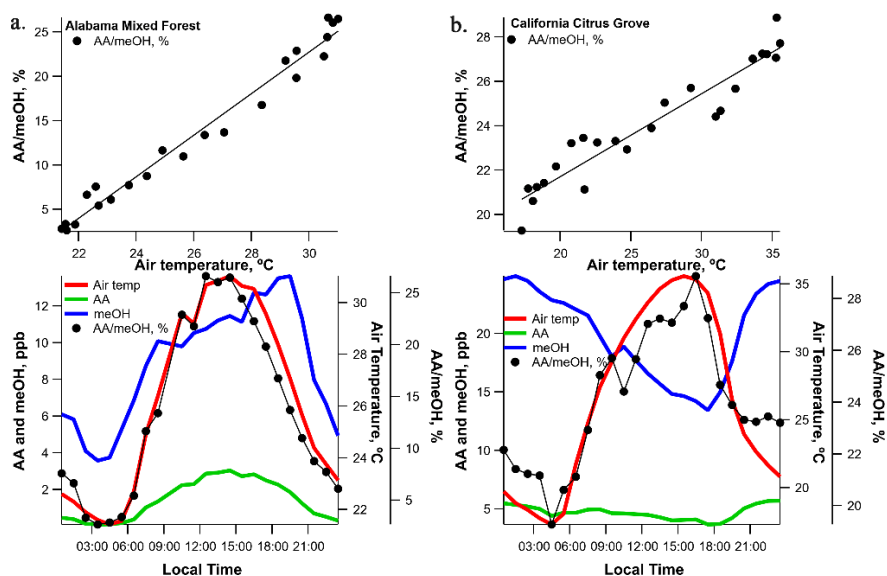


**Figure 9 :** Average diurnal MeOH and AA concentrations and AA/MeOH ratios together with air temperature during the growing season above (a) a mixed forest in Alabama, USA (Suet *et al.*, 2016) and (b) a citrus grove in California, USA (Parket *et al.*, 2013) during the growing season. Average diurnal MeOH (blue) and AA (green) ambient concentrations with air temperature together with AA/MeOH concentration ratios are plotted.

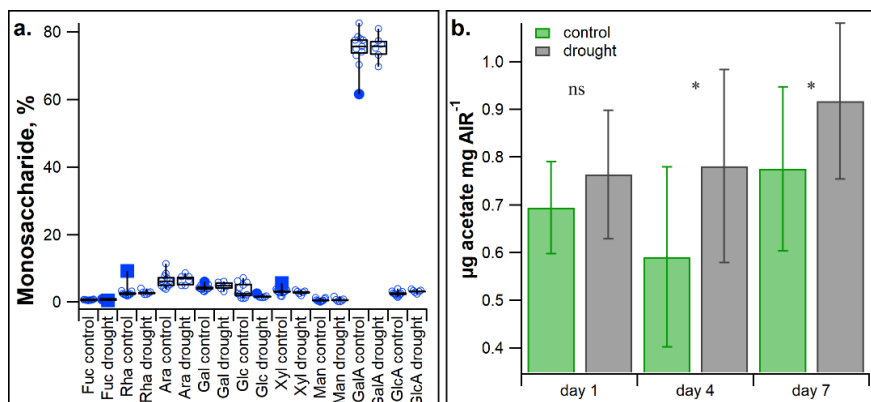


**Figure 10:** **a.** Leaf bulk cell wall monosaccharide composition from control and drought stressed poplar trees one day following cessation of soil moisture additions. Monosaccharides quantified are fucose (Fuc), rhamnose (Rha), arabinose (Ara), galactose (Gal), glucose (Glc), xylose (Xyl), mannose (Man), galacturonic acid (GalA) and glucuronic acid (GlcA). **b.** Also shown are leaf bulk cell wall *O*-acetyl methyl ester content released following saponification of alcohol insoluble residue (AIR) preparations of control and drought stressed leaves on day 1, 4, and 7 of the drought. Values are plotted as average  $\pm$  one standard deviation (ns indicates no statistical significance between control and drought treatments, \* indicates statistically significant differences,  $P < 0.05$ ). Note, no statistically significant differences were observed in monosaccharide composition between control and drought treatments during days 1, 4, or 7.

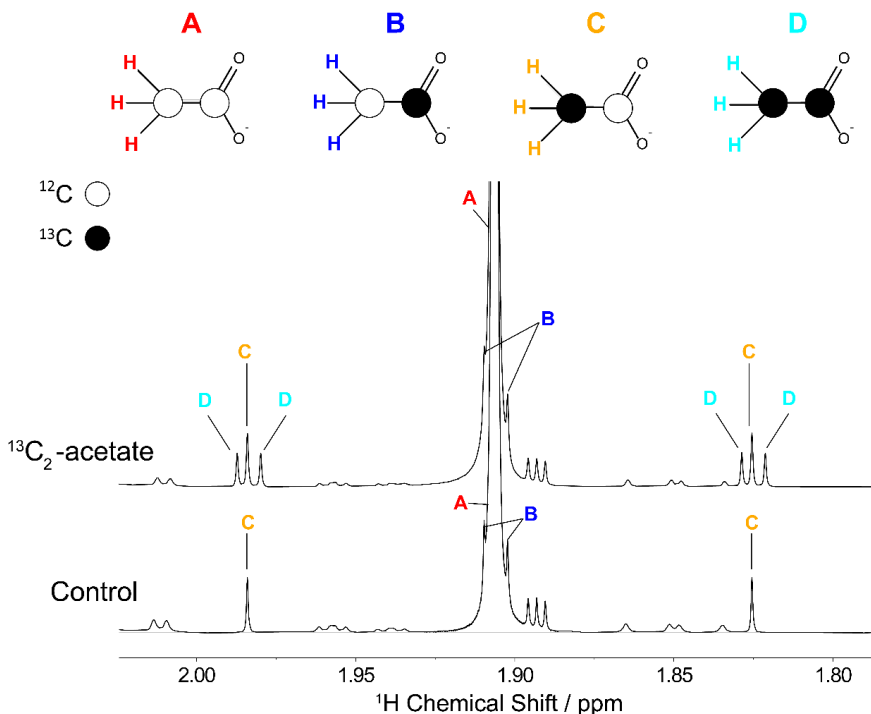


**Figure 11 :** Exploring the mechanism of leaf bulk cell wall *O*-acetylation. Simplified schematic showing acetate and its four-stable carbon isotopologues with 0 (**A**), 1 (**B** and **C**), and 2 (**D**)  $^{13}\text{C}$  atoms. Following delivery of a 10 mM  $^{13}\text{C}_2$ -acetate to detached poplar branches and a whole poplar tree via the transpiration stream, leaf cell walls were isolated and analyzed by  $^1\text{H}$ -NMR. Note: the much more intense  $^{12}\text{C}_2$ -

isotopologue signal (A) was clipped vertically in both control and  $^{13}\text{C}_2$ -acetate spectra to show the details of the satellite peaks corresponding to the remaining isotopologues which are labeled B-D.

## Acknowledgements

This material is based upon work supported by the U.S. Department of Energy (DOE), Office of Science, Office of Biological and Environmental Research (BER), Biological System Science Division (BSSD), Early Career Research Program under Award number FP00007421 to Lawrence Berkeley National Laboratory. This work was also supported as part of the DOE Joint BioEnergy Institute through contract DE-AC02-05CH11231 to Lawrence Berkeley National Laboratory. A portion of this research was performed on project awards (10.46936/cpcy.proj.2019.50708/60006566 and 10.46936/expl.proj.2019.51078/60006676) from the Environmental Molecular Sciences Laboratory, a DOE Office of Science User Facility sponsored by the BER program under Contract No. DE-AC05-76RL01830. We would like to acknowledge extensive project guidance from Eoin Brodie and Christina Wistrom for the maintenance and establishment of our poplar trees at the UC Berkeley Oxford Greenhouse. In addition, we would like to acknowledge Thomas Powell for practical advice on leaf water potential measurements and the helpful discussions on cell wall elasticity and plant drought stress responses.

## References

- Ahl L.I., Mravec J., Jørgensen B., Rudall P.J., Rønsted N. & Grace O.M. (2019) Dynamics of intracellular mannan and cell wall folding in the drought responses of succulent Aloe species. *Plant, Cell & Environment* **42**, 2458–2471.
- Amsbury S., Hunt L., Elhaddad N., Baillie A., Lundgren M., Verhertbruggen Y., ... Gray J.E. (2016) Stomatal Function Requires Pectin De-methyl-esterification of the Guard Cell Wall. *Current Biology* **26**, 2899–2906.
- An S.H., Sohn K.H., Choi H.W., Hwang I.S., Lee S.C. & Hwang B.K. (2008) Pepper pectin methylesterase inhibitor protein CaPMEI1 is required for antifungal activity, basal disease resistance and abiotic stress tolerance. *Planta* **228**, 61–78.
- Aulia M.R., Liyantono, Setiawan Y. & Fatikhunnada A. (2016) Drought detection of west java's paddy field using MODIS EVI satellite images (case study: rancaekek and rancaekek wetan). *Procedia Environmental Sciences* **33**, 646–653.
- Biely P. (2012) Microbial carbohydrate esterases deacetylating plant polysaccharides. *Biotechnology advances* **30**, 1575–1588.
- Braybrook S.A., Hofte H. & Peaucelle A. (2012) Probing the mechanical contributions of the pectin matrix: insights for cell growth. *Plant Signaling & Behavior* **7**, 1037–1041.
- Chebli Y. & Geitmann A. (2017) Cellular growth in plants requires regulation of cell wall biochemistry. *Current Opinion in Cell Biology* **44**, 28–35.
- Derbyshire P., McCann M.C. & Roberts K. (2007) Restricted cell elongation in Arabidopsis hypocotyls is associated with a reduced average pectin esterification level. *BMC Plant Biology* **7**, 31.
- Dewhirst R.A., Afseth C.A., Castanha C., Mortimer J.C. & Jardine K.J. (2020b) Cell wall O-acetyl and methyl esterification patterns of leaves reflected in atmospheric emission signatures of acetic acid and methanol. *Plos One* **15**, e0227591.
- Dewhirst R.A., Handakumbura P., Clendinen C.S., Arm E., Tate K., Wang W., ... Jardine K.J. (2021a) High Temperature Acclimation of Leaf Gas Exchange, Photochemistry, and Metabolomic Profiles in *Populus trichocarpa*. *ACS Earth and Space Chemistry*.
- Dewhirst R.A., Mortimer J.C. & Jardine K.J. (2020a) Do cell wall esters facilitate forest response to climate? *Trends in Plant Science* **25**, 729–732.

- Dewhirst R.A., Lei J., Afseth C.A., Castanha C., Wistrom C.M., Mortimer J.C., Jardine K.J. (2021b) Are Methanol-Derived Foliar Methyl Acetate Emissions a Tracer of Acetate-Mediated Drought Survival in Plants?. *Plants*. 2021 Feb 23;10(2):411.
- Eamus D., Boulain N., Cleverly J. & Breshears D.D. (2013) Global change-type drought-induced tree mortality: vapor pressure deficit is more important than temperature per se in causing decline in tree health. *Ecology and Evolution* **3**, 2711–2729.
- Fall R. (2003) Abundant oxygenates in the atmosphere: a biochemical perspective. *Chemical Reviews* **103**, 4941–4952.
- Furtado A., Lupoi J.S., Hoang N.V., Healey A., Singh S., Simmons B.A. & Henry R.J. (2014) Modifying plants for biofuel and biomaterial production. *Plant Biotechnology Journal* **12**, 1246–1258.
- Ganie S.A. & Ahammed G.J. (2021) Dynamics of cell wall structure and related genomic resources for drought tolerance in rice. *Plant Cell Reports***40**, 437–459.
- Gille S. & Pauly M. (2012) O-acetylation of plant cell wall polysaccharides. *Frontiers in plant science* **3**, 12.
- Gou J.-Y., Miller L.M., Hou G., Yu X.-H., Chen X.-Y. & Liu C.-J. (2012) Acetyltransferase-mediated deacetylation of pectin impairs cell elongation, pollen germination, and plant reproduction. *The Plant Cell***24**, 50–65.
- Harley, P., Greenberg, J., Niinemets, Ü. and Guenther, A., 2007. Environmental controls over methanol emission from leaves. *Biogeosciences* , **4** ( **6** ), 1083-1099.
- Helm L.T., Shi H., Lerdau M.T. & Yang X. (2020) Solar-induced chlorophyll fluorescence and short-term photosynthetic response to drought. *Ecological Applications* **30**, e02101.
- Hong M.J., Kim D.Y., Lee T.G., Jeon W.B. & Seo Y.W. (2010) Functional characterization of pectin methyltransferase inhibitor (PMEI) in wheat. *Genes & Genetic Systems* **85**, 97–106.
- Hüve K., Christ M.M., Kleist E., Uerlings R., Niinemets U., Walter A. & Wildt J. (2007) Simultaneous growth and emission measurements demonstrate an interactive control of methanol release by leaf expansion and stomata. *Journal of Experimental Botany* **58**, 1783–1793.
- Jardine K., Karl T., Lerdau M., Harley P., Guenther A., Mak J.E. Carbon isotope analysis of acetaldehyde emitted from leaves following mechanical stress and anoxia. (2009) *Plant Biology***11**(**4**) , 591-7.
- Jardine K.J., Chambers J.Q., Holm J., Jardine A.B., Fontes C.G., Zorzanelli R.F., ... Manzi A.O. (2015) Green Leaf Volatile Emissions during High Temperature and Drought Stress in a Central Amazon Rainforest. *Plants* **4**, 678–690.
- Jardine K.J., Fernandes de Souza V., Oikawa P., Higuchi N., Bill M., Porras R., ... Chambers J.Q. (2017) Integration of C1 and C2 metabolism in trees. *International Journal of Molecular Sciences* **18**, 2045.
- Jardine K.J., Jardine A.B., Souza V.F., Carneiro V., Ceron J.V., Gimenez B.O., ... Chambers J.Q. (2016) Methanol and isoprene emissions from the fast-growing tropical pioneer species *Vismia guianensis* (Aubl.) Pers. (Hypericaceae) in the central Amazon forest. *Atmospheric Chemistry and Physics* **16**, 6441–6452.
- Jardine K.J., Sommer E.D., Saleska S.R., Huxman T.E., Harley P.C., Abrell L. Gas phase measurements of pyruvic acid and its volatile metabolites. (2010) *Environmental Science & Technology*. **44** ( **7** ), 2454-60.
- Jardine K., Yañez Serrano A, Arneth A, Abrell L, Jardine A, Artaxo P, Alves E, Kesselmeier J, Taylor T, Saleska S, Huxman T. (2011) Ecosystem-scale compensation points of formic and acetic acid in the central Amazon. *Biogeosciences* **8** ( **12** ), 3709-20.
- Ji Y., Zhou G., Li Z., Wang S., Zhou H. & Song X. (2020) Triggers of widespread dieback and mortality of poplar (*Populus* spp.) plantations across northern China. *Journal of arid environments* **174**, 104076.

- Kim J.-M., To T.K., Matsui A., Tanoi K., Kobayashi N.I., Matsuda F., ... Seki M. (2017) Acetate-mediated novel survival strategy against drought in plants. *Nature Plants* **3**, 17097.
- Kreuzwieser J., Scheerer U. & Rennenberg H. (1999) Metabolic origin of acetaldehyde emitted by poplar (*Populus tremula* x *P. alba*) trees. *Journal of experimental botany* **50**, 757–765.
- Lefebvre V., Fortabat M.-N., Ducamp A., North H.M., Maia-Grondard A., Trouverie J., ... Durand-Tardif M. (2011) ESKIMO1 disruption in *Arabidopsis* alters vascular tissue and impairs water transport. *Plos One* **6**, e16645.
- Levesque-Tremblay G., Pelloux J., Braybrook S.A. & Müller K. (2015) Tuning of pectin methylesterification: consequences for cell wall biomechanics and development. *Planta* **242**, 791–811.
- Liu Y., Zhou R., Wen Z., Khalifa M., Zheng C., Ren H., ... Wang Z. (2021) Assessing the impacts of drought on net primary productivity of global land biomes in different climate zones. *Ecological Indicators* **130**, 108146.
- McDowell N., Pockman W.T., Allen C.D., Breshears D.D., Cobb N., Kolb T., ... Yezzer E.A. (2008) Mechanisms of plant survival and mortality during drought: why do some plants survive while others succumb to drought? *The New Phytologist* **178**, 719–739.
- Millerd A., Bonner J. Acetate activation and acetoacetate formation in plant systems. (1954) *Archives of Biochemistry and Biophysics*, **49** (2), 343-55.
- Mohnen D. (2008) Pectin structure and biosynthesis. *Current Opinion in Plant Biology* **11**, 266–277.
- Novaković L., Guo T., Bacic A., Sampathkumar A. & Johnson K.L. (2018) Hitting the Wall-Sensing and Signaling Pathways Involved in Plant Cell Wall Remodeling in Response to Abiotic Stress. *Plants* **7**, 89.
- Orfila C., Dal Degan F., Jørgensen B., Scheller H.V., Ray P.M. & Ulvskov P. (2012) Expression of mung bean pectin acetyl esterase in potato tubers: effect on acetylation of cell wall polymers and tuber mechanical properties. *Planta* **236**, 185–196.
- Palut M. & Canziani O.F. (2007) Contribution of working group II to the fourth assessment report of the intergovernmental panel on climate change.
- Park J.H., Goldstein A.H. & Timkovsky J. (2013) Eddy covariance emission and deposition flux measurements using proton transfer reaction–time of flight–mass spectrometry (PTR-TOF-MS): comparison with PTR-MS measured vertical gradients and fluxes. *Atmospheric Chemistry and Physics*, **13**, 1439-1456.
- Pathre U., Sinha A.K., Shirke P.A. & Sane P.V. (1998) Factors determining the midday depression of photosynthesis in trees under monsoon climate. *Trees* **12**, 472.
- Pauly M. & Keegstra K. (2010) Plant cell wall polymers as precursors for biofuels. *Current Opinion in Plant Biology* **13**, 305–312.
- Pauly M. & Scheller H.V. (2000) O-Acetylation of plant cell wall polysaccharides: identification and partial characterization of a rhamnogalacturonan O-acetyl-transferase from potato suspension-cultured cells. *Planta* **210**, 659–667.
- Peaucelle A., Braybrook S. & Höfte H. (2012) Cell wall mechanics and growth control in plants: the role of pectins revisited. *Frontiers in plant science* **3**, 121.
- Peaucelle A., Braybrook S.A., Le Guillou L., Bron E., Kuhlemeier C. & Höfte H. (2011) Pectin-induced changes in cell wall mechanics underlie organ initiation in *Arabidopsis*. *Current Biology* **21**, 1720–1726.
- Peaucelle A., Louvet R., Johansen J.N., Höfte H., Laufs P., Pelloux J. & Mouille G. (2008) *Arabidopsis* phyllotaxis is controlled by the methyl-esterification status of cell-wall pectins. *Current Biology* **18**, 1943–1948.

- Peters A.J., Walter-Shea E.A., Ji L. & Vina A. (2002) Drought monitoring with NDVI-based standardized vegetation index. . . . *and remote sensing*.
- Portillo-Estrada M., Zenone T., Arriga N. & Ceulemans R. (2018) Contribution of volatile organic compound fluxes to the ecosystem carbon budget of a poplar short-rotation plantation. *Global change biology. Bioenergy* **10**, 405–414.
- Ragauskas A.J., Williams C.K., Davison B.H., Britovsek G., Cairney J., Eckert C.A., . . . Tschaplinski T. (2006) The path forward for biofuels and biomaterials. *Science* **311**, 484–489.
- Ramírez V., Xiong G., Mashiguchi K., Yamaguchi S. & Pauly M. (2018) Growth- and stress-related defects associated with wall hypoacetylation are strigolactone-dependent. *Plant Direct* **2**, e00062.
- Rasheed S., Bashir K., Kim J.-M., Ando M., Tanaka M. & Seki M. (2018) The modulation of acetic acid pathway genes in Arabidopsis improves survival under drought stress. *Scientific Reports* **8**, 7831.
- Ren A., Ahmed R.I., Chen H., Han L., Sun J., Ding A., . . . Kong Y. (2019) Genome-Wide Identification, Characterization and Expression Patterns of the Pectin Methyltransferase Inhibitor Genes in Sorghum bicolor. *Genes* **10**.
- Roig-Oliver M., Nadal M., Clemente-Moreno M.J., Bota J. & Flexas J. (2020) Cell wall components regulate photosynthesis and leaf water relations of Vitis vinifera cv. Grenache acclimated to contrasting environmental conditions. *Journal of Plant Physiology* **244**, 153084.
- Sannigrahi P., Ragauskas A.J. & Tuskan G.A. (2010) Poplar as a feedstock for biofuels: A review of compositional characteristics. *Biofuels, Bioproducts and Biorefining* **4**, 209–226.
- Scheller H.V. (2017) Plant cell wall: Never too much acetate. *Nature Plants* **3**, 17024.
- Sechet J., Htwe S., Urbanowicz B., Agyeman A., Feng W., Ishikawa T., . . . Mortimer J.C. (2018) Suppression of Arabidopsis GGLT1 affects growth by reducing the L-galactose content and borate cross-linking of rhamnogalacturonan-II. *The Plant Journal: for Cell and Molecular Biology* **96**, 1036–1050.
- de Souza A., Hull P.A., Gille S. & Pauly M. (2014) Identification and functional characterization of the distinct plant pectin esterases PAE8 and PAE9 and their deletion mutants. *Planta* **240**, 1123–1138.
- Su L., Patton E.G., Vilà-Guerau de Arellano J., Guenther A.B., Kaser L., Yuan B., . . . Mak J.E. (2016) Understanding isoprene photooxidation using observations and modeling over a subtropical forest in the southeastern US. *Atmospheric Chemistry and Physics* **16**, 7725–7741.
- Sun Y., Fu R., Dickinson R., Joiner J., Frankenberg C., Gu L., . . . Fernando N. (2015) Drought onset mechanisms revealed by satellite solar-induced chlorophyll fluorescence: Insights from two contrasting extreme events. *Journal of Geophysical Research: Biogeosciences* **120**, 2427–2440.
- Tadege M. (1997) Aerobic fermentation during tobacco pollen development. *Plant Molecular Biology* . **35** (3), 343–54.
- Trueba S., Pan R., Scoffoni C., John G.P., Davis S.D. & Sack L. (2019) Thresholds for leaf damage due to dehydration: declines of hydraulic function, stomatal conductance and cellular integrity precede those for photochemistry. *The New Phytologist* **223**, 134–149.
- Willats W.G., McCartney L., Mackie W. & Knox J.P. (2001) Pectin: cell biology and prospects for functional analysis. *Plant Molecular Biology* **47**, 9–27.
- Yuan Y., Teng Q., Zhong R., Haghghat M., Richardson E.A. & Ye Z.-H. (2016) Mutations of arabidopsis TBL32 and TBL33 affect xylan acetylation and secondary wall deposition. *Plos One* **11**, e0146460.
- Zhong R., Cui D. & Ye Z.-H. (2017) Regiospecific Acetylation of Xylan is Mediated by a Group of DUF231-Containing O-Acetyltransferases. *Plant & Cell Physiology* **58**, 2126–2138.

Zhou J., Zhang Z., Sun G., Fang X., Zha T., McNulty S., ... Noormets A. (2013) Response of ecosystem carbon fluxes to drought events in a poplar plantation in Northern China. *Forest Ecology and Management* **300**, 33–42.

